

# Mining for Peace\*

Roland Hodler<sup>†</sup>      Paul Schaudt<sup>‡</sup>      Alberto Vesperoni<sup>§</sup>

July 2024

## Abstract

We study the feasibility of opening new mines in ethnically diverse, low-income countries without escalating the risk of conflict. We propose a theoretical model in which ethnic groups can organize themselves to fight at the national or the local level. Our model yields two key insights. First, peace cannot be guaranteed in the presence of ethnic segregation and spatial resource inequality. Second, once the peace maximizing policies are implemented, local conflict risks depend on local resource rents and local ethnic groups as well as the country's entire ethnic and mining geography. We validate key concepts from our model using granular spatial data and shift-share identification strategies. Finally, we apply these concepts to simulate the potential impact of planned mining projects in Sierra Leone. We confirm that projects in the right locations can promote peace and discuss policy recommendations for making the mining industry a facilitator of peace and prosperity.

*Key words:* Civil conflict, ethnic conflict, natural resources, mining, ethnic segregation.

---

\*We are thankful for helpful comments by James Fenske, Kai Gehring, Victoire Girard, Pierre-Guillaume Méon, Massimo Morelli, and Dominic Rohner; conference participants at the African Meeting of the Econometric Society, the Bari Conference on the Economics of Global Interactions, the European Development Economics Network, the European Public Choice Conference, the Nordic Conference in Development Economics, the Swiss Development Economics Conference, and the Swiss Society of Economics and Statistics Conference; as well as seminar participants at King's College London, the University of Lucerne, the University of St.Gallen, and the Wyss Academy. Paul Schaudt acknowledges funding from the Swiss National Science Foundation Ambizione project PZ00P1208916.

<sup>†</sup>Department of Economics, University of St.Gallen; CEPR; CESifo; OxCarre; email: roland.hodler@unisg.ch.

<sup>‡</sup>Department of Economics, University of St.Gallen; email: paul.schaudt@unisg.ch.

<sup>§</sup>Department of Political Economy, King's College London; email: alberto.vesperoni@kcl.ac.uk.

# 1 Introduction

Global demand for minerals is rising, presenting development opportunities for resource-rich countries in Africa and beyond. Unfortunately, the exploitation of natural resources has often fuelled ethnic conflicts (e.g., [Berman et al., 2017](#)), causing misery in the countries producing and exporting minerals. It is crucial to develop strategies that allow low-income countries to effectively mitigate mining-related conflict risks. These strategies would help them capitalize on the current opportunities and could guarantee a stable supply of critical minerals required for the green energy transition.

We present novel theoretical arguments and corroborating empirical evidence suggesting that the spatial distribution of industrial mining sites is a key determinant of mining-related conflict. We argue that the effect of new mines on conflict risks depends on the location of these new mines as well as the country's entire mining and ethnic geographies (i.e., the location and revenues of its existing mines and the spatial distribution of its ethnic populations). The link between the local and the national level arises from the possibility of members of a group forming intra-ethnic coalitions at the local or at the national level and, therefore, bargain for resource rents at both levels simultaneously.<sup>1</sup> We show that peace cannot be guaranteed in the presence of ethnic segregation and spatial resource inequality, but that there often exist mining projects in locations where new mining activities reduce the country's overall conflictuality – a possibility to which we refer as *mining for peace*. Moreover, we provide theoretical concepts for quantifying conflict-related externalities of new mines and discuss how policymakers and mining companies could use these concepts, e.g., for the proper pricing of mining licenses or human rights due diligence.

**Theoretical contribution:** Our first contribution is a theoretical model to predict the occurrence and location of conflict events as a function of the observed spatial distributions of natural resource rents and ethnic groups. Our model features a country with an arbitrary distribution of ethnic groups and resource rents across locations.<sup>2</sup> Ethnic groups constitute coalitions that can contend resource rents at the local level (in conflicts that involve their local populations fighting

---

<sup>1</sup>The interaction between local and national (or more generally, systemic) factors is at the center of our methodology and broadly in line with general principles of social network theory. For complementary applications to the economics of conflict see, e.g., [König et al. \(2017\)](#) and [Amarasinghe et al. \(2020\)](#).

<sup>2</sup>Like many others, we are interested in the role of politically relevant identities and employ ethnicity as an empirical proxy for identity.

for the local resource rents) or at the national level (in a grand conflict that involves their whole ethnic group fighting for the entire pool of resource rents). The possibility of different intra-ethnic coalitions links the local and the national level, and the resulting possibility of conflict at different levels can lead to bargaining failure (as in [Morelli and Rohner, 2015](#)).<sup>3</sup>

Following the general suggestion of [Roth \(2002\)](#), we take a mechanism-design approach and study a central planner that prioritizes the implementation of peace at the national level while simultaneously attempting to minimize local conflict risks.<sup>4</sup>

To do so, the planner can redistribute resource rents across ethnic groups and locations under uncertainty of the private conflict costs of the groups involved. The resulting conflict risks metaphorically represent the least conflictual outcome that could be achieved in bargaining between local and national leaders of ethnic groups in the shadow of conflict. Hence, these risks can be seen as lower bounds; they would increase in the presence of political economy constraints on efficient bargaining.<sup>5</sup> We are agnostic on the means by which the planner redistributes resource rents but notice that discriminatory taxation, politically targeted transfers, biased local public goods provision, and unequal employment opportunities are common in many countries.

We first show that the implementation of peace (at the national level and in all locations) via the truthful revelation of such costs is generally impossible in the presence of ethnic segregation and spatial resource inequality, thus linking the occurrence of local conflicts to country-level systemic properties. We then characterize the probability of conflict at each location when the planner implements the (second-best) transfer scheme that guarantees peace at the national level and minimizes local conflict risks based on prior information only. These predictions for local conflict risks are a main difference to [Morelli and Rohner \(2015\)](#), along

---

<sup>3</sup>The argument that there needs to be a bargaining failure for conflict to occur goes back to [Fearon \(1995\)](#). [Jackson and Morelli \(2011\)](#) and [Blattman \(2022\)](#) discuss different types of bargaining failures.

<sup>4</sup>For earlier work on conflict outbreak relying on mechanism design, see, e.g., [Bester and Wärneryd \(2006\)](#), [Fey and Ramsay \(2009\)](#), and [Hörner et al. \(2015\)](#). Information asymmetries are the leading force for understanding conflict outbreak in these approaches. Relatedly, [Laurent-Lucchetti et al. \(2024\)](#) present a model in which free and fair elections can reduce information asymmetries between ethnic groups and, thereby, reduce the risk of conflict. In contrast, conflict typically occurs even in the absence of any information asymmetry in our model, while the presence of information asymmetry augments the parameter range for which it does.

<sup>5</sup>The planner could alternatively represent a government with strong preferences to avoid conflict, in particular, conflict at the national level. After all, national conflicts are usually associated with higher costs for society and pose higher risks for the political survival of governments and leaders of ethnic groups than (more limited) local conflict.

with the mechanism design framework, the arbitrary number of ethnic groups and locations, and the broader set of potential conflict initiators at the local as well as the national level.

More generally, our model offers a nuanced narrative on the role of ethnicity in conflicts over natural resources. Instead of assuming that all ethnic groups are inclined to fight for resource rents, there is an endogenous politicization and violent radicalization along ethnic lines. It is the groups that are generally over-represented in resource-rich locations that get politicized and radicalized. [Berman et al. \(2023\)](#) document that these ethnic groups often feel economically deprived and politically excluded. Our model implies that these groups experience “discord” between high local resource rents and their comparatively low post-transfer well-being. Members of such discordant groups may thus initiate local conflicts.

Importantly, the model delivers two prominent indices for empirical analysis: the national *peace deficit* and the local *conflict exposure*. The former corresponds to the monetary amount that would be necessary to guarantee peace everywhere, which is our proxy for the country’s aggregate propensity for conflict. The latter is a proxy for the relative propensity for conflict at each location.

**Empirical contribution:** Our second contribution is to provide empirical support for our theoretical model by validating that a higher national peace deficit and higher local conflict exposure indeed coincide with higher levels of national and local conflict. Our main analysis focuses on Sierra Leone, for which we can obtain granular data on conflict locations and the location and size of mines as well as census data on local ethnic diversity. Moreover, we test the predictions of our model in a wider set of West African countries using less granular data on local ethnic diversity.

We validate the theoretical predictions on local conflict exposure in different ways. First, following the static nature of the model, we time-average the data over the entire sample period as well as different sub-periods (characterized by the economic importance of different minerals). Second, we make use of the panel dimension and run standard two-way fixed effects regressions as well as two-stage least squares regressions with a generated instrument based on a shift-share approach that is commonly used in literature to deal with potentially endogenous mining operations (e.g., [Bazzi and Blattman, 2014](#); [Berman and Couttenier, 2015](#); [Berman et al., 2017](#); [Dube and Vargas, 2013](#)). These different empirical analyses all show a close relation between the theoretically predicted local conflict exposure and the observed local conflict risks. Results are qualitatively similar in our larger West Africa sample.

Turning to the national level, we document a strong correlation between the theoretically derived peace deficit and the observed aggregate propensity for conflict over time. Taken together, our empirical analyses suggest that our theoretical model is able to predict how – conditional on a country’s ethnic geography – changes in its mining geography shape the occurrence and location of conflict events.

Our empirical contribution provides further nuance to the literature on the effects of natural resources and ethnic diversity on conflict.<sup>6</sup> In particular, our framework allows us to focus on the systemic component of the local conflict risk that depends on a country’s entire ethnic and mining geography while accounting for local determinants of local conflict. Thus, we build a bridge between cross-country studies (e.g., [Collier and Hoeffler, 2004](#)) and granular spatial studies (e.g., [Adhvaryu et al., 2021](#); [Berman et al., 2017](#)) on natural resources, ethnic diversity, and conflict.

**Policy contribution:** Our third contribution is to use the theoretical concepts of the national peace deficit and the local conflict exposure to simulate the consequences of new industrial mining projects. We consider all known mineral deposits in Sierra Leone and run counterfactual analyses to predict how the hypothetical development of these deposits would affect the overall risk of conflict and the spatial distribution thereof. For example, we predict that the planned new gold mines on the Baomahun and Nimini deposits would increase the country’s aggregate propensity for conflict. Importantly, we also identify alternative (gold) deposits whose development would lower the aggregate propensity for conflict. Hence, we confirm that *mining for peace* is not only a theoretical but also an empirical possibility. We also document that these hypothetical mining projects would have very different effects on the spatial distribution of local conflict risks. We illustrate this heterogeneity by focusing on the effects on the local conflict risk around these deposits as well as the local conflict risk around currently active industrial mines.

We view the changes in local and aggregate conflict risks induced by new mining projects as externalities. We propose that governments and other stakeholders

---

<sup>6</sup>See, e.g., [Collier and Hoeffler \(2004\)](#), [Humphreys \(2005\)](#), [Brückner and Ciccone \(2010\)](#), [Dube and Vargas \(2013\)](#), [Bazzi and Blattman \(2014\)](#), [Lei and Michaels \(2014\)](#), [Berman et al. \(2017\)](#) and [Hodler et al. \(2023\)](#) on the role of natural resources; [Montalvo and Reynal-Querol \(2005\)](#), [Matuszeski and Schneider \(2006\)](#), [Esteban and Ray \(2008\)](#), [Desmet et al. \(2012\)](#), [Esteban et al. \(2012\)](#), [Esteban et al. \(2015\)](#), [Corvalan and Vargas \(2015\)](#), [Novta \(2016\)](#), [Spolaore and Wacziarg \(2016\)](#), [Desmet et al. \(2017\)](#), [Eberle et al. \(2020\)](#) and [McGuirk and Nunn \(2024\)](#) on the role of ethnic diversity; and [Morelli and Rohner \(2015\)](#), [Adhvaryu et al. \(2021\)](#) and [Gehring et al. \(2023\)](#) on the interaction between the two.

use the concepts of the national peace deficit and the local conflict exposure to conduct cost-benefit analyses when designing mining policies. Explicitly considering the conflict externalities generated by new mines allows for better assessment of the true costs of mining in specific locations and allows for pricing mining licenses properly. Thus, we contribute to a recent literature that discusses policies to mitigate the political resource curse, such as public information campaigns (Armand et al., 2020), foreign corruption regulation (Christensen et al., 2024), and international certification schemes (Binzel et al., 2024). In addition, our framework also offers insights for international mining companies, not least because conflict threatens their assets, increases their production and transportation costs, and undermines their “social licenses to operate,” which have become common in the mining industry (e.g., Prno and Slocombe, 2012).

The remainder of the paper is structured as follows. Section 2 present our theoretical model. Section 3 introduces our empirical setting and data. Section 4 provides empirical support for our theoretical concepts, and Section 5 applies them in counterfactual analyses to study how new mining projects would affect conflict. Section 6 concludes and provides policy recommendations for making the mining industry a facilitator of peace and prosperity in the Global South.

## 2 Model

Consider a country that is inhabited by a continuum of individuals. This population is partitioned into a finite set of ethnic groups  $G \subset \mathbb{N}$  and a finite set of locations  $L \subset \mathbb{N}$ . These locations may represent subnational administrative or political units like wards in Sierra Leone. We denote the mass of individuals in ethnic group  $g \in G$  and location  $l \in L$  by  $m_l^g \geq 0$ , with  $m_l := \sum_{g \in G} m_l^g$ ,  $m^g := \sum_{l \in L} m_l^g$ , and  $m := \sum_{g \in G} m^g$ .

Mining activities and the associated upstream and downstream services give rise to resource rents. The resource rent in location  $l \in L$  is  $r_l > 0$ , where  $r := \sum_{l \in L} r_l$  denotes the aggregate resource rent and  $\mathbf{r}$  their  $|L|$  dimensional vector. Individuals can form intra-ethnic coalitions at the local or the national level to contend resource rents in conflicts at the local or the national level, respectively.<sup>7</sup>

In case of local or national conflict, a fraction of the corresponding resources is

---

<sup>7</sup>We refrain from allowing for a wider set of admissible coalitions, e.g., inter-ethnic coalitions, but the consequences on the theoretical results are relatively clear. Augmenting the set of admissible coalitions would render conflict more likely, thereby strengthening the impossibility results in Propositions 1 and 2, while weakening our predictive capacity in Proposition 3.

used to fight or destroyed in the conflict, while the rest is preserved. The groups' forecasts of these preserved fractions (perhaps mediated by psychological factors such as pride and entitlement) determine their valuations of the spoils of victory. As such fractions are difficult to assess due to unpredictable conflict dynamics of winners and losers, we think of them as subjective, thus random and privately known. We denote by  $v_l^g \in [0, 1]$  the fraction of the local resource rent  $r_l$  that the local representatives of group  $g \in G$  believe to be preserved in case of a conflict they win in location  $l \in L$  (their local valuation). Similarly, we denote by  $v^g$  the fraction of the national resource rent  $r$  that the national representatives of group  $g \in G$  believe to be preserved in case of a national conflict they win (their national valuation). The groups' subjective valuations of victory are then represented by a  $|G| \times (|L| + 1)$  dimensional matrix  $\mathbf{v}$  with  $v_l^g$  and  $v^g$  as typical elements.

In case of conflict in location  $l \in L$ , the expected aggregate payoff of the local members of ethnic group  $g \in G$  is thus  $r_l v_l^g s_l^g$ , where  $s_l^g \in [0, 1]$  denotes the expected share of preserved local resource rent conquered by them. Similarly, in case of national conflict, the expected aggregate payoff of members of ethnic group  $g \in G$  in the whole country is  $r v^g s^g$ , where  $s^g \in [0, 1]$  denotes the expected share of preserved aggregate resource rent conquered by them. In line with the literature, we think of  $s_l^g$  and  $s^g$  as winning probabilities in winner-take-all conflicts, so that naturally  $\sum_{g \in G} s_l^g = 1$  for each  $l \in L$  and  $\sum_{g \in G} s^g = 1$ . The distribution of these expected shares is represented by a  $|G| \times (|L| + 1)$  dimensional matrix  $\mathbf{s}$  with  $s_l^g$  and  $s^g$  as typical elements.

In the theoretical literature on conflict, the expected shares  $\mathbf{s}$  are typically modeled as winning probabilities determined by the strategic interaction of the competing groups in conflict, where both group sizes and mobilization motives matter in determining the relative strength of a group. While the former can be directly determined by demography, i.e., the population shares of the ethnic groups (which may be considered exogenous in the short to medium run), the latter are complex and jointly determined by, among others, the salience of ethnic identity, the complementarity of labor and capital in collective action, and the incentives of leaders and followers (e.g., [Atkin et al., 2021](#); [Esteban and Ray, 2008](#); [Jackson and Morelli, 2007](#)). In our model we abstract from such complex motives and simply assume that the expected shares are determined by the demographic representation of ethnic groups, so that they are proportional to their population shares in the relevant context, i.e.,  $s_l^g = m_l^g / m_l$  and  $s^g = m^g / m$ .<sup>8</sup>

---

<sup>8</sup>This assumption implies that we abstract from modeling fighting efforts and that all groups are equally efficient in converting population mass into military strength. One could easily

The focus of our analysis is instead on the promotion of peace via transfers of resource rents across ethnic groups and locations. For this purpose, we consider a planner who can redistribute resource rents to implement peace both at the local and the national level. As discussed in the Introduction, the planner could metaphorically represent the efficient bargaining between leaders of ethnic groups in the shadow of conflict.<sup>9</sup> The focus on resource rents implies that the planner can transfer the income generated by the resource endowments but not the endowments themselves. In this setting, the transfer received by a group determines the group's payoff under peace: specifically, the aggregate payoff for members of ethnic group  $g \in G$  in location  $l \in L$  in case of peace at location  $l$  is their transfer  $t_l^g \geq 0$ , while the aggregate payoff of the whole ethnic population of group  $g \in G$  in case of peace at the national level is their aggregate transfer  $t^g := \sum_{l \in L} t_l^g$ . A system of transfers is denoted by a  $|G| \times |L|$  dimensional matrix  $\mathbf{t}$  with  $t_l^g$  as a typical element.

The objective of the planner is to promote peace in the highest number of locations while guaranteeing peace at the national level. Hence, the planner first and foremost aims to avoid the outbreak of a national conflict, e.g., because the consequences are particularly uncertain and potentially detrimental for both the political leadership and the entire country. Moreover, as locations may not be equally important to the planner, we assign a priority weight  $w_l \in (0, 1)$  to each location  $l \in L$ , with  $\sum_{l \in L} w_l = 1$ .<sup>10</sup> We assume the planner maximizes the weighted sum of the peace probabilities  $p_l \in [0, 1]$  across all locations,

$$\max_{\mathbf{t}} \sum_{l \in L} w_l p_l, \quad (1)$$

subject to guaranteeing peace at the national level, a budget constraint, and in-

---

modify this assumption and let some groups, say those in power, be more efficient in this regard. In addition, we could also assume that some groups have exclusive access to some resource rents that other groups cannot contend. Recent empirical work by [Morelli et al. \(2024\)](#) shows that population size is indeed a major factor predicting the fighting efficacy of groups.

<sup>9</sup>The resulting conflict risks metaphorically represent the least conflictual outcomes that could be achieved with bargaining and transfers when local and national conflicts are simultaneous threats. In presence of additional constraints on efficient bargaining due to political economy factors external to our model, the resulting conflict risks would necessarily be higher.

<sup>10</sup>We introduce these weights in the planner's objective to demonstrate the flexibility and portability of our approach across different institutional and political contexts. These weights could represent, e.g., a preference for peace in locations with active mining sites or the presence of ethno-regional favoritism ([Burgess et al., 2015](#); [De Luca et al., 2018](#); [Hodler and Raschky, 2014](#)) when thinking of the planner as a country's president. We acknowledge that these weights can be difficult to measure empirically and do not attempt to do so in this paper (as they do not appear in theoretical concepts that we bring to the data).

formational frictions. We call such objective *peace maximizing*. We will carry this objective across all stages of our theoretical inquiry in slightly different forms, adapted to the specific informational structure.<sup>11</sup>

In our model, the crucial friction for peace is that transfers represent the status-quo income of the groups (their peace payoff) and thus cannot be conditioned on the local or national nature of the conflict threat. Instead, the transfers should prevent conflict at both levels at the same time, as ethnic coalitions may mobilize at either the local or the national level after the transfers are determined.<sup>12</sup> On top of this commitment friction on the side of the groups, the planner has two fundamental constraints for promoting peace. The first is the limited budget for redistribution, which is determined by the aggregate value of the resource rents. The second is the limited information about the groups' perceptions of the wastefulness of conflict, as quantified by  $v^g$  and  $v_l^g$ , which are privately known by the groups.

In the course of our analysis, we will consider three alternative ways the planner may approach the latter (informational) constraint. In Section 2.1, we study the conditions under which the planner can guarantee peace at the national level and all locations – thus achieving the *unconstrained maximum* of the planner's objective (1) – for any possible realization of  $\mathbf{v}$  and, therefore, in the absence of any reliable knowledge on  $\mathbf{v}$ . This exercise delivers a restrictive condition for peace implementation (the *peace condition*), the set of groups that initiate conflict (the *discordant groups*), and the amount of additional funds necessary to pacify the country (the *peace deficit*).

In Section 2.2, we inquire whether the constrained maximum of (1) can be reached via a system of transfers that incentivizes the groups to truthfully reveal their private information on  $v_l^g$  and  $v^g$ . We find that such a transfer system fails to exist whenever the peace condition is violated, thus suggesting a general impossibility.

Finally, in Section 2.3, we study the constrained maximum of (1) based on

---

<sup>11</sup>The linear specification of the planner's objective is consistent with Von Neumann–Morgenstern representation of the planner's preferences in the form of expected utility, where the weight  $w_l$  represents the difference between the utility of peace and the utility of conflict in location  $l$ .

<sup>12</sup>If groups were ex-ante committed to a type of conflict – with ethnic coalitions mobilizing either at the local or national level – conflict could always be prevented via an opportune transfer system that redistributes the peace surplus by rewarding coalitions proportionally to their strength. This, however, fails to occur in our model in which groups can choose to mobilize either at the local or national level after they learn their status-quo incomes. For related approaches where, despite efficient bargaining and transfers, conflict occurs due to commitment frictions, see Ray (2009) and Morelli and Rohner (2015).

prior information only (rather than revealed information). As a result of this analysis, we obtain the probability of conflict at each location, which is the central prediction of our model.

## 2.1 Peace guaranteeing transfers

In this section, we inquire whether the planner can achieve the *unconstrained maximum* of the peace maximizing objective (1) in the absence of reliable knowledge and, therefore, for any  $\mathbf{v}$ .

As in all our model specifications, the planner will attempt to do so by appropriately redistributing resource rents. We, therefore, introduce some terminology that will carry on in subsequent sections. First, given  $\mathbf{r}$ , we say that a system of transfers  $\mathbf{t}$  is *budget feasible* if  $\sum_{g \in G} t^g \leq r$ . This condition requires the planner's intervention to be purely redistributive and does not allow for extra income. Second, given  $\mathbf{r}$  and  $\mathbf{s}$ , we say that a system of transfers  $\mathbf{t}$  *guarantees peace everywhere* if, for every possible  $\mathbf{v}$ , it does so simultaneously at the national level and in each location, i.e.,

$$t^g \geq s^g r v^g \text{ and } t_l^g \geq s_l^g r_l v_l^g \text{ for each } g \in G \text{ and } l \in L.$$

These conditions are very restrictive as they must hold even for the most demanding case of non-destructive conflicts (i.e.,  $v_l^g = v^g = 1$ ). They can be seen as the ideal goal of a planner who, fearing the chaotic consequences of conflict, aims at guaranteeing peace at every level and every location under any foreseeable contingency.

We are now ready to state our first result that characterizes the *peace condition*, i.e., the narrow set of configurations of  $\mathbf{r}$  and  $\mathbf{s}$  that can guarantee peace everywhere in a budget-feasible manner.

**Proposition 1** *Given  $\mathbf{r}$  and  $\mathbf{s}$ , there exists a system of transfers  $\mathbf{t}$  that guarantees peace everywhere and is budget feasible if and only if*

$$1 = \sum_{l \in L} (r_l/r) (s_l^g / s^g) \text{ for each } g \in G. \quad (2)$$

*Proof:* Take any  $\mathbf{r}$  and  $\mathbf{s}$ . It is immediate that there exists such a system of transfers if and only if peace can be feasibly implemented when  $v_l^g = v^g = 1$  for each  $l \in L$  and  $g \in G$ . Suppose this is the case. Guaranteed peace everywhere requires  $t^g \geq r s^g$  and  $t_l^g \geq r_l s_l^g$  for each  $g \in G$  and  $l \in L$ . Budget feasibility

requires  $r \geq \sum_{g \in G} t^g$ , which given the above implies  $t^g = rs^g$  for all  $g \in G$  and  $t_l^g = r_l s_l^g$  for each  $g \in G$  and  $l \in L$ .  $\mathbf{t}$  satisfies these two properties if and only if  $t^g = rs^g$  and  $t_l^g = r_l s_l^g$  for each  $g \in G$  and  $l \in L$ . Given  $t^g = \sum_{l \in L} t_l^g$ , we can then conclude that such  $\mathbf{t}$  exists if and only if  $rs^g = \sum_{l \in L} r_l s_l^g$  for each  $g \in G$ , which is equivalent to (2).  $\square$

Given that the expected shares take the form  $s_l^g = m_l^g/m_l$  and  $s^g = m^g/m$  for all  $l \in L$  and  $g \in G$ , it is straightforward that the peace condition (2) can be rewritten as

$$1 = \sum_{l \in L} (r_l/r) [(m_l^g/m_l)/(m^g/m)] \quad \text{or} \quad 1 = \sum_{l \in L} [(r_l/m_l)/(r/m)] (m_l^g/m^g).$$

Hence, it holds in two special cases: First, it holds if there is no ethnic segregation, i.e., if  $m_l^g/m_l = m^g/m$  for all  $l \in L$  and  $g \in G$ , as understood from the first equality. Second, it holds if there is no inequality in per capita resource rents across locations, i.e., if  $r_l/m_l = r/m$  for all  $l \in L$ , as understood from the second equality. However, in the presence of ethnic segregation and spatial resource inequality the peace condition (2) does not generally hold. Hence, peace cannot typically be guaranteed.

[Figure 1](#) illustrates these insights with a series of simple examples. Panel A shows a country with no spatial resource inequality. There, a peace guaranteeing, budget-feasible transfer scheme exists because per-capita resource rents are identical across locations. Panel B shows a country with no ethnic segregation. There, such a transfer scheme exists because each group's population share is identical across locations. In contrast, peace cannot typically be guaranteed in all countries like the one shown in Panel C where there is both ethnic segregation and spatial resource inequality.<sup>13</sup>

We now take a closer look at why conflict emerges. Importantly, conflict may only be initiated by groups belonging to the set

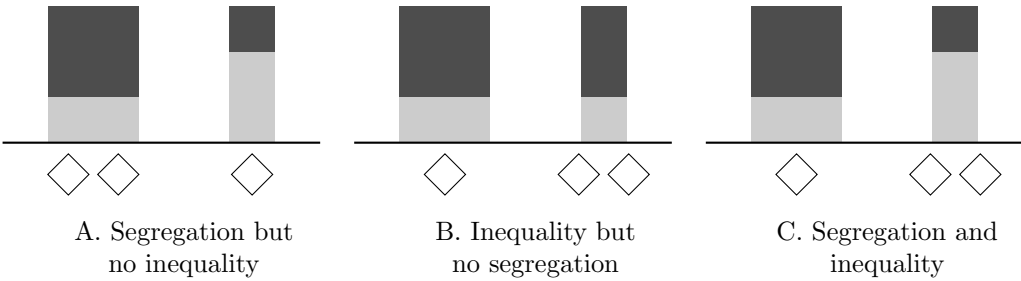
$$G^* = \{g \in G : 1 < \sum_{l \in L} (r_l/r) (s_l^g/s^g)\}. \quad (3)$$

This definition can be easily understood in relation to the peace condition (2). Intuitively, if peace is guaranteed at the national level for every  $\mathbf{v}$ , the aggregate transfers to groups must equal their maximum claims at the national level,  $t^g =$

---

<sup>13</sup>For the case with two locations and two ethnic groups, the absence of spatial inequality *or* ethnic segregation is a necessary and sufficient condition for peace implementation. With more groups or more locations instead, this presence is only a sufficient condition.

FIGURE 1  
Illustration of peace condition



*Notes:* Each graph represents a different country where the horizontal axis represents different locations  $l \in L = \{1, 2\}$  and each tone of gray indicates a different ethnic group  $g \in G = \{1, 2\}$ . The size of the gray rectangular areas above the horizontal axis indicates the population mass  $m_l^g$  of each group  $g \in G$  in each location  $l \in L$ . The diamonds below the horizontal axis indicate the resource rent  $r_l$  at each location  $l \in L$ .

$s^g r$ . Then, the groups that may initiate local conflict are the ones that are over-represented in locations that are resource-rich. The reason is that they are short of transfers from the constraint at the national level:

$$rs^g = t^g = \sum_{l \in L} t_l^g < \sum_{l \in L} r_l s_l^g.$$

Hence, they may experience discord between these resource rents accruing in the locations where they predominately live and their comparatively low post-transfer well-being. We, therefore, call the groups in set  $G^*$  *discordant groups*. All other groups  $g \notin G^*$  are over-represented in locations that are resource-poor so that their total transfers  $t^g = s^g r$  are more than sufficient to ensure they do not initiate conflict in any location,  $t_l^g \geq s_l^g r_l$ .

To see an example of the logic of discordant groups, consider again Figure 1. There, the set of discordant groups is empty in all panels but Panel C, which we already identified as the only case of conflict. In this panel, the group depicted in light gray is a discordant group as it is over-represented in the resource-rich location on the right. The other group, instead, depicted in dark gray, is non-discordant as it is under-represented in this location.

We conclude this section by defining a measure of the general tendency for conflict in a country. We call this measure the *peace deficit*, as it quantifies the amount of additional funds that would allow the planner to guarantee peace everywhere. By Proposition 1 and the related discussion of discordant groups, it is straightfor-

ward that the peace deficit can be written as

$$\Delta := \sum_{g \in G} \max \left\{ \sum_{l \in L} r_l s_l^g - rs^g, 0 \right\} = \sum_{g \in G^*} \left( \sum_{l \in L} r_l s_l^g - rs^g \right). \quad (4)$$

Intuitively,  $\Delta = 0$  if the peace condition holds – which also implies that the set of discordant groups is empty – while  $\Delta > 0$  otherwise. In our empirical application to Sierra Leone, we will use the peace deficit  $\Delta$  as a measure of the country’s aggregate propensity for conflict.

## 2.2 Peace implementing mechanism

In this section, we discuss whether the constrained maximum of the peace maximizing objective (1) can be reached via a system of transfers that incentivizes the groups to truthfully reveal their private information on  $v_l^g$  and  $v^g$ .

The desirability of such information revelation is straightforward. Having established that it is (generally impossible) to guarantee peace for every possible realization of  $\mathbf{v}$ , we now consider whether the planner can promote peace for at least some of these realizations. More specifically, conflict could always be prevented if known to be very destructive, e.g., if  $v_l^g \approx 0$  and  $v^g \approx 0$  for all  $g$  and  $l$ , as relatively low transfers would be sufficient to guarantee that all groups opt for peace. Thus, if the planner was able to identify such realizations of  $\mathbf{v}$ , it could at least guarantee peace in contingencies where conflict is particularly wasteful. This, however, is not immediate as the perceived wastefulness of conflict – as measured by  $v_l^g$  and  $v^g$  – is private information of the groups, and groups may not have an incentive to truthfully communicate this to the planner.

Taking a mechanism design approach, we focus on the scenario in which the members of group  $g \in G$  inhabiting each location  $l \in L$  are required to reveal their perceived preserved fraction  $v_l^g \in [0, 1]$  to the planner via a corresponding message  $\mu_l^g \in [0, 1]$ , while the national representatives of group  $g$  are required to reveal  $v^g \in [0, 1]$  via  $\mu^g \in [0, 1]$ . In this context, a mechanism is a function  $T$  that maps each profile of messages  $\mu := (\mu_l^g, \mu^g)$  into the corresponding transfer system  $t_l^g = T_l^g(\mu)$  for each  $l \in L$  and  $g \in G$ , where  $t^g = \sum_{l \in L} T_l^g(\mu)$ .<sup>14</sup> Given the transfer system is implemented, all groups act upon their transfer and their perceived preserved fractions  $v_l^g$  and  $v^g$ . Hence, there is conflict outbreak at location  $l \in L$

---

<sup>14</sup>The extension to stochastic mechanisms – mapping message profiles into probability distributions over transfer systems – is omitted for ease of exposition but straightforward, leading to the same impossibility conclusions below.

if and only if  $t_l^{g'} < s_l^{g'} r_l v_l^{g'}$  for some  $g' \in G$ , and national conflict outbreak if and only if  $t^{g'} < s^{g'} r v^{g'}$  for some  $g' \in G$ .

We consider two desirable properties that a mechanism should satisfy for every given profile of preserved fractions  $\mathbf{v}$ . Adapting (1) to the present setting, we say that a mechanism is *peace maximizing* (PM) if it implements peace at the national level and, given that this is guaranteed, implements peace at the local level for the highest ( $w_l$ -weighted) number of locations. Borrowing a conventional idea from the literature, we say that a mechanism is *incentive compatible* (IC) if the national and local representatives of each group have a weak incentive to truthfully reveal their private information to the planner whenever peace is implemented by such revelation in the relevant (national or local) context.<sup>15</sup> We are now ready to state our next result:

**Proposition 2** *Given  $\mathbf{r}$  and  $\mathbf{s}$ , there exists a mechanism that is peace maximizing and incentive compatible if and only if the peace condition (2) holds.*

*Proof:* Suppose  $\mathbf{r}$  and  $\mathbf{s}$  take any value such that the peace condition (2) holds. Then, it is straightforward that the simple mechanism  $T_l^g(\mathbf{v}) = s_l^g r_l$  for each  $g \in G$  and  $l \in L$  satisfies PM and IC. Now, suppose  $\mathbf{r}$  and  $\mathbf{s}$  take any value such that (2) does not hold. We want to show that either PM or IC must be violated for some  $\mathbf{v}$ . We start by showing that, at the national level, it is impossible to extract truthful information unless the budget is exhausted. To see this, consider any pair of valuation profiles  $\mathbf{v}$  and  $\mathbf{u}$  with  $v^g < u^g \leq 1$  for some  $g \in G$ . As by PM peace is prioritized and thus always guaranteed at the national level, by IC we must have  $\sum_{l \in L} T_l^g(\mathbf{v}) = \sum_{l \in L} T_l^g(\mathbf{u})$  or the national representative of group  $g$  would have an incentive to misreport either  $v^g$  or  $u^g$ . Then, PM and IC jointly require  $\sum_{l \in L} T_l^g(\mu^g, \mathbf{v}^{\neg g}) = s^g r$  for all  $\mu^g \in [0, 1]$  and  $g \in G$ . Having established this, we continue our analysis by considering the behavior of groups' local representatives. Take any type profile  $\mathbf{v}$  and group  $g' \in G$  such that  $s^{g'} r = \sum_{l \in L} r_l s_l^{g'} v_l^{g'}$  so that the budget is just enough to guarantee group  $g'$  is peaceful at each location. The existence of such  $g'$  - which is necessarily a discordant group - is guaranteed by the violation of the peace condition (2). By PM we must have  $T_l^{g'}(\mathbf{v}) = s_l^{g'} r_l v_l^{g'}$  for all  $l \in L$ , which combined with IC leads to  $T_l^{g'}(\mathbf{v}) = s_l^{g'} r_l v_l^{g'} \geq T_l^{g'}(v_l^{g'} + \epsilon, \mathbf{v}_{\neg l}^{\neg g'})$  for all  $l \in L$  and  $\epsilon > 0$ . Consider the alternative profile  $\mathbf{u}$  such that  $u_l^{g'} = v_l^{g'} + \epsilon$  for some

---

<sup>15</sup>Let  $\mathbf{v}_{\neg l}^{\neg g}$  denote the restriction of  $\mathbf{v}$  to all elements other than the representatives of group  $g \in G$  in location  $l \in L$ , and  $\mathbf{v}^{\neg g}$  the restriction of  $\mathbf{v}$  to all elements other than the national representatives of group  $g \in G$ . Formally,  $T$  is IC if, for each  $l \in L$  and  $g \in G$ ,  $T_l^g(\mathbf{v}) \geq T_l^g(\mu_l^g, \mathbf{v}_{\neg l}^{\neg g})$  for any  $\mu_l^g \in [0, 1]$  when  $T_l^{g'}(\mathbf{v}) \geq s_l^{g'} r_l v_l^{g'}$  for all  $g' \in G$ , and  $\sum_{l \in L} T_l^g(\mathbf{v}) \geq \sum_{l \in L} T_l^g(\mu^g, \mathbf{v}^{\neg g})$  for any  $\mu^g \in [0, 1]$  when  $\sum_{l \in L} T_l^{g'}(\mathbf{v}) \geq s^{g'} r v^{g'}$  for all  $g' \in G$ .

$l' \in L$  and  $\epsilon > 0$  while  $u_l^{g'} = v_l^{g'}$  for all  $l \neq l'$ . Note that  $s^{g'}r < \sum_{l \in L} r_l s_l^{g'} u_l^{g'}$ , so group  $g'$  is necessarily conflictual in some location under  $\mathbf{u}$ . Suppose  $\epsilon$  is arbitrarily small so that by PM conflict is prevented in all locations but one, and without loss of generality let  $l'$  be among the peaceful locations. Then, by IC we must have  $T_{l'}^{g'}(\mathbf{u}) = T_{l'}^{g'}(v_{l'}^{g'} + \epsilon, \mathbf{v}_{\neg l'}^{g'}) \geq s_{l'}^{g'} r_{l'}(v_{l'}^{g'} + \epsilon)$ , which is a contradiction as  $\epsilon$  is assumed positive.  $\square$

Proposition 1 has shown that peace can be guaranteed in the absence of information revelation only in the narrow set of cases satisfying the peace condition (2). Now, Proposition 2 shows that peace implementation is limited to the identical set of cases. Communication of private information thus fails to promote peace whenever relevant, making Proposition 2 effectively an *impossibility result*. We conclude that informational frictions make conflict generally unavoidable even when it is so wasteful that (in principle) there are enough transfers to convince all groups to sustain peace. The intuition for the impossibility of truthful revelation is that local groups may have an incentive to pretend being short of transfers when they are not. This pretense is to the advantage of the group's representatives in the location that claims the shortage of transfers but against the interest of the remaining group members that face an increased exposure to conflict outbreak in other locations. Note that, as peace is prioritized at the national level, the transfers to each group are fixed in aggregate and information is used to determine how they should be distributed across the group's local representatives. At its core, the impossibility of truthful revelation is thus a collective action problem within groups.

## 2.3 Constrained optimization and local conflict exposure

In this section, we study the planner's constrained optimization of the peace maximizing objective (1) based on prior information only (rather than no information or revealed information, as in the previous two sections). As a result, we will obtain the probability of conflict at each location under the implementation of the optimal transfer system.

In line with our general assumptions on the planner's objective (1) and constraints, we assume that – for each resource distribution  $\mathbf{r}$  and group strength distribution  $\mathbf{s}$  that violate the peace condition (2) – the planner chooses the transfer scheme  $\mathbf{t}$  to maximize the expected ( $w_l$ -weighted) number of peaceful locations

subject to ensuring peace at the national level:

$$\max_{\mathbf{t}} \sum_{l \in L} w_l p_l(\mathbf{t}_l, \mathbf{s}_l, r_l) \text{ s.t. } t^g = s^g r \text{ for each } g \in G.$$

The probability of peace at each location  $l \in L$ ,  $p_l(\mathbf{t}_l, \mathbf{s}_l, r_l)$ , is determined by the commonly known prior distribution of perceived fractions of preserved resources at the local level,  $v_l^1, \dots, v_l^{|G|}$ , which for simplicity we assume to be independent across locations. For the sake of tractability, we also assume that these fractions are independently and identically distributed within locations, according to a cumulative distribution function  $\Phi : [0, 1] \rightarrow [0, 1]$ .<sup>16</sup> Again, we assume that group  $g \in G$  at location  $l \in L$  acts upon the perceived fraction  $v_l^g$  and thus refrains from starting local conflict if and only if  $t_l^g \geq s_l^g r_l v_l^g$ . As peace has to be sustained unanimously, the probability of peace at location  $l \in L$  can thus be written as

$$p_l(\mathbf{t}_l, \mathbf{s}_l, r_l) = \prod_{g \in G} \Phi(\min\{t_l^g / (s_l^g r_l), 1\})$$

and the corresponding probability of conflict as  $c_l(\mathbf{t}_l, \mathbf{s}_l, r_l) = 1 - p_l(\mathbf{t}_l, \mathbf{s}_l, r_l)$ . We propose that  $\Phi$  should be increasing, differentiable and concave, implying a decreasing density function. Such density functions capture the idea that preserved fractions are hard to predict but that highly wasteful events are comparatively more likely – perhaps due to the infamous reputation of ethnic conflicts. The power form  $\Phi(x) = x^\alpha$  with  $\alpha \in (0, 1)$  satisfies these properties and, for  $\alpha$  sufficiently small, turns out to be particularly convenient to obtain an explicit solution.

We are now ready to state our result. As we are ultimately interested in an explicit formula for the risk of conflict  $c_l(\mathbf{t}_l, \mathbf{s}_l, r_l)$  that can be used in the empirical application, we thereby focus on *interior solutions*, i.e., configurations of  $\mathbf{r}$  and  $\mathbf{s}$  such that, given the optimal transfer scheme is in place, each discordant group has a positive probability of initiating conflict in each location.<sup>17</sup>

**Proposition 3** *Let  $\Phi(x) = x^\alpha$  with  $\alpha \in (0, 1/|G^*|)$ . If the optimal system of transfers  $\mathbf{t}^*$  is implemented and the solution interior, the probability of conflict at*

---

<sup>16</sup>These independence assumptions are necessary to obtain closed-form solutions that we can bring to the data. We will empirically confirm that these solutions are helpful to predict the occurrence of local conflict events. The lack of generality (due to these assumptions) may however limit the normative value of the second-best transfer scheme derived below.

<sup>17</sup>The focus on interior solutions is necessary for tractability and to get a closed-form solution that we can bring to the data. Given the arbitrary number of groups and locations (and corresponding parameters) in this model, the possibilities for different configurations of corner solutions are infinite.

each location  $l \in L$  is

$$c_l(\mathbf{t}_l^*, \mathbf{s}_l, r_l) = 1 - \frac{(w_l)^{|G^*|\alpha/(1-\alpha|G^*|)} e_l(\mathbf{t}_l^*, \mathbf{s}_l, r_l)^{-|G^*|\alpha/[1-|G^*|\alpha]} }{[\sum_{l' \in L} (w_{l'})^{1/(1-\alpha|G^*|)} e_{l'}(\mathbf{t}_{l'}^*, \mathbf{s}_{l'}, r_{l'})^{-|G^*|\alpha/[1-|G^*|\alpha]}]^{1/|G^*|}},$$

where the local conflict exposure is

$$e_l(\mathbf{t}_l^*, \mathbf{s}_l, r_l) := (r_l/r) \left[ \prod_{g \in G^*} (s_l^g/s^g) \right]^{1/|G^*|}. \quad (5)$$

*Proof:* The planner's problem is equivalent to the unconstrained maximization of the following Lagrangian with respect to  $\mathbf{t}$  and the vector of multipliers  $\lambda := (\lambda_1, \dots, \lambda_{|G|})$ ,

$$\mathcal{L}(\mathbf{t}, \lambda) = \sum_{l \in L} \prod_{g \in G} w_l \Phi(\min\{t_l^g/(s_l^g r_l), 1\}) + \sum_{g \in G} \lambda^g (s^g r - \sum_{l \in L} t_l^g).$$

It is immediate that  $\lambda_g = 0$  for each group  $g \notin G^*$ , as by (3) for any of them  $t^g = rs^g \geq \sum_{l \in L} r_l s_l^g$  and we can thus guarantee they do not initiate conflict in any location  $l \in L$  by setting  $t_l^g \geq r_l s_l^g$ . From now on we then focus on the groups within set  $G^*$  and assume an interior solution. By the definition of interior solution, all groups in  $G^*$  have a chance to initiate conflict in each location, which implies  $\lambda^g > 0$  and  $\sum_{l \in L} t_l^g = s^g r$  for each  $g \in G^*$ . For each  $l' \in L$  and  $g' \in G^*$ , the first-order condition for the optimality of  $t_{l'}^{g'}$  is

$$\frac{\Phi'(t_{l'}^{g'}/(s_{l'}^{g'} r_{l'}))}{s_{l'}^{g'} r_{l'}} \prod_{g \in G^* \setminus \{g'\}} \Phi(t_{l'}^g/(s_{l'}^g r_{l'})) = \lambda_{g'}/w_{l'},$$

which leads to

$$\frac{\Phi(t_{l'}^{g'}/(s_{l'}^{g'} r_{l'}))}{\Phi'(t_{l'}^{g'}/(s_{l'}^{g'} r_{l'}))} s_{l'}^{g'} r_{l'} = \frac{w_{l'}}{\lambda_{g'}} p_{l'}(\mathbf{t}_{l'}, \mathbf{s}_{l'}, r_{l'}).$$

Given  $\Phi(x) = x^\alpha$  with  $\alpha \in (0, 1/|G^*|)$ , we can write  $(t_{l'}^{g'}/\alpha) = (w_{l'}/\lambda_{g'}) p_{l'}(\mathbf{t}_{l'}, \mathbf{s}_{l'}, r_{l'})$ . By  $s^g r = \sum_{l' \in L} t_{l'}^g$  we then obtain  $\lambda_{g'} = [\alpha/(s^g r)] \sum_{l \in L} w_l p_l(\mathbf{t}_l, \mathbf{s}_l, r_l)$ , and thus

$$\frac{t_{l'}^{g'}}{s^{g'} r} = \frac{w_{l'} p_{l'}(\mathbf{t}_{l'}, \mathbf{s}_{l'}, r_{l'})}{\sum_{l \in L} w_l p_l(\mathbf{t}_l, \mathbf{s}_l, r_l)} = \frac{w_{l'} \prod_{g \in G^*} (t_{l'}^g/(s_{l'}^g r_{l'}))^\alpha}{\sum_{l \in L} w_l \prod_{g \in G^*} (t_l^g/(s_l^g r_l))^\alpha}. \quad (6)$$

It follows that  $t_l^g/t_{l'}^{g'} = (w_l/w_{l'}) [p_l(\mathbf{t}_l, \mathbf{s}_l, r_l)/p_{l'}(\mathbf{t}_{l'}, \mathbf{s}_{l'}, r_{l'})]$  for all  $g \in G^*$  and  $l, l' \in$

$L$ , which leads to

$$\frac{p_l(\mathbf{t}_l, \mathbf{s}_l, r_l)}{p_{l'}(\mathbf{t}_{l'}, \mathbf{s}_{l'}, r_{l'})} = \frac{\prod_{g \in G^*} (t_l^g / (s_l^g r_l))^{\alpha}}{\prod_{g \in G^*} (t_{l'}^g / (s_{l'}^g r_{l'}))^{\alpha}} = \left[ \frac{p_l(\mathbf{t}_l, \mathbf{s}_l, r_l)}{p_{l'}(\mathbf{t}_{l'}, \mathbf{s}_{l'}, r_{l'})} \right]^{\alpha |G^*|} \left[ \frac{w_l}{w_{l'}} \right]^{\alpha |G^*|} \left[ \frac{r_l}{r_{l'}} \right]^{-\alpha |G^*|} \left[ \frac{\prod_{g \in G^*} s_l^g}{\prod_{g \in G^*} s_{l'}^g} \right]^{-\alpha}$$

and therefore to

$$\frac{w_{l'} p_{l'}(\mathbf{t}_{l'}, \mathbf{s}_{l'}, r_{l'})}{\sum_{l \in L} w_l p_l(\mathbf{t}_l, \mathbf{s}_l, r_l)} = \frac{(w_{l'})^{1/(1-\alpha|G^*|)} \left[ (r_{l'}/r)^{|G^*|} \prod_{g \in G^*} (s_{l'}^g / s^g) \right]^{-\alpha/(1-|G^*|\alpha)}}{\sum_{l \in L} (w_l)^{1/(1-\alpha|G^*|)} \left[ (r_l/r)^{|G^*|} \prod_{g \in G^*} (s_l^g / s^g) \right]^{-\alpha/(1-|G^*|\alpha)}}.$$

By (6), the transfer to each group  $g \in G^*$  in location  $l' \in L$  is then

$$t_{l'}^g = s^g r \frac{(w_{l'})^{1/(1-\alpha|G^*|)} \left[ (r_{l'}/r)^{|G^*|} \prod_{g \in G^*} (s_{l'}^g / s^g) \right]^{-\alpha/(1-|G^*|\alpha)}}{\sum_{l \in L} (w_l)^{1/(1-\alpha|G^*|)} \left[ (r_l/r)^{|G^*|} \prod_{g \in G^*} (s_l^g / s^g) \right]^{-\alpha/(1-|G^*|\alpha)}},$$

and given  $p_{l'}(\mathbf{t}_{l'}, \mathbf{s}_{l'}, r_{l'}) = \prod_{g \in G^*} (t_{l'}^g / (s_{l'}^g r_{l'}))^{\alpha}$ , the probability of peace in  $l' \in L$  is

$$p_{l'}(\mathbf{t}_{l'}, \mathbf{s}_{l'}, r_{l'}) = \frac{(w_{l'})^{|G^*|\alpha/(1-\alpha|G^*|)} \left[ (r_{l'}/r)^{|G^*|} \prod_{g \in G^*} (s_{l'}^g / s^g) \right]^{-\alpha/(1-|G^*|\alpha)}}{\left[ \sum_{l \in L} (w_l)^{1/(1-\alpha|G^*|)} \left[ (r_l/r)^{|G^*|} \prod_{g \in G^*} (s_l^g / s^g) \right]^{-\alpha/(1-|G^*|\alpha)} \right]^{|G^*|\alpha}}.$$

The corresponding probability of conflict is  $c_{l'}(\mathbf{t}_{l'}, \mathbf{s}_{l'}, r_{l'}) = 1 - p_{l'}(\mathbf{t}_{l'}, \mathbf{s}_{l'}, r_{l'})$ .  $\square$

Proposition 3 delivers the principal testable prediction of our model. In particular, we expect a high correlation between the theoretically predicted local conflict risk  $c_l$  and the observed frequency of local conflict events. This conflict risk  $c_l$  is decreasing in the priority weight  $w_l$  that the planner assigns to location  $l$  and increasing in the local conflict exposure  $e_l$ . The priority weight may well capture some known local determinants of local conflict, such as the presence of active mines or the share of the president's co-ethnics residing in a given ward. These are likely mediated by the preferences of who is in power and thus, at least partly, subjective. In contrast,  $e_l$  captures the more systemic (and arguably, more nuanced) effects of the country's entire ethnic and mining geography on local conflict, which are the main focus of our analysis and, from our perspective, more objectively quantifiable. In our empirical analysis, we will thus focus on the local conflict exposure  $e_l$  while controlling for some known local determinants of local conflict.<sup>18</sup>

---

<sup>18</sup>The local conflict exposure  $e_l$  is not a probability, as it abstracts from average effects on a country's propensity for conflict across locations. Such average effects are instead captured by the denominator of  $c_l$  (which is a measure of the dispersion of the distribution of the priority

We now briefly discuss the determinants and structure of the local conflict exposure  $e_l$ . By its definition (5), the local conflict exposure – and, therefore, the corresponding conflict risk – depends on the interplay of two complementary forces. The first is the relative presence of *contestable resources*,  $(r_l/r)$ . The second is the geometric mean of the discordant groups’ relative population shares,  $D_{l,G^*} := \left[ \prod_{g \in G^*} (s_l^g / s^g) \right]^{1/|G^*|}$ , which can be interpreted as a measure of local ethnic diversity quantifying the discordant groups’ over-representation in the location.<sup>19</sup> As this measure depends on the population shares of discordant groups only, it captures these groups’ *endogenous radicalization* as well as the *bargaining failure* that results from their claims at various levels of spatial aggregation. The complementarity of these forces is captured by the multiplicative form of the conflict exposure index:  $e_l = (r_l/r)D_{l,G^*}$ .

We empirically validate our conflict prediction (5) in the next sections. Moreover, it accounts for several prominent stylized facts in the literature: First, conflict events often occur in resource-rich locations (e.g., [Berman et al., 2017](#)). Second, conflict events often occur in ethnically diverse locations of segregated countries (e.g., [Corvalan and Vargas, 2015](#); [Eberle et al., 2020](#); [Matuszeski and Schneider, 2006](#); [McGuirk and Nunn, 2024](#)). Third, ethnic groups in resource-rich locations often feel economically deprived and politically excluded ([Berman et al., 2023](#)). Our prediction systematizes these stylized facts and emphasizes their complementarities, which is essential for understanding the systemic effects of mining.

### 3 Setting and data

In this section, we provide some background information about Sierra Leone and introduce our granular spatial data from Sierra Leone as well as our main variables. In Appendix C, we introduce less granular spatial data for a sample of eight West African countries and test the external validity of our Sierra Leone-based results.

---

weights and the local conflict exposures) or, more conveniently, by the peace deficit  $\Delta$ , which has the added advantages of being independent of the unknown priority weights, our independence assumptions, and our focus on interior solutions. Nevertheless, the local conflict exposure is perfectly valid and practically convenient to understand within-country variation in the relative propensity for conflict.

<sup>19</sup>The interpretation of  $D_{l,G^*}$  as a measure of ethnic diversity follows from the application of the (inverse of) the principle of transfers in inequality measurement to fractionalization measures, as  $D_{l,G^*}$  increases whenever population is marginally transferred from a locally larger to a locally smaller discordant ethnic group.

### 3.1 Sierra Leone

Sierra Leone is an ethnically diverse country of 8 million people. There are several sizeable ethnic groups, many of which are still over-represented in their traditional homelands. Mineral mining has a long tradition in Sierra Leone. It started on a large scale during the British colonial period in the 1930s with the founding of the Sierra Leone Development Company, which obtained the rights to mine iron in Marampa, where there is still a large iron mine as of 2023. Sierra Leone became independent in 1961. The first few years after independence were characterized by peace and economic growth. However, soon politics was dominated by ethnic tensions, coups, a switch to a one-party constitution, the violent suppression of the opposition, and kleptocratic tendencies within the elite.

The Sierra Leonean civil war started in 1991 when the Revolutionary United Front (RUF) invaded out of neighboring Liberia. The government of Sierra Leone and its army (SLA) were unable to react decisively, and the conflict spread over the entire country. Outright battles between the SLA and the RUF were the exception. Instead, the primary targets of violence were civilians and, in case of RUF, local chiefs. The inability of the government to defend communities led to the formation of Community Defence Forces (CDF), mostly consisting of civilians and traditional hunter groups ([Bellows and Miguel, 2006](#)). A UN intervention led by the United Kingdom ended the civil war in 2002. In total, more than 50,000 people were killed in this war ([Bellows and Miguel, 2006](#); [Kaldor and Vincent, 2006](#)).

Diamonds played a crucial role in the financing of all organized armed forces. All industrial mining operations came to a halt after the beginning of the civil war, but diamonds could easily be mined with forced labor and little capital and could be illicitly exported ([Bellows and Miguel, 2009](#)).

Despite the politicization of ethnic identities and the ethnicization of political processes in post-independence Sierra Leone ([Kandeh, 1992](#)), ethnic identities do not seem to have played a central role in the civil war in the form of grievances ([Bellows and Miguel, 2006](#)). While initial recruitment within the CDF followed ethnic lines to some degree ([Bellows and Miguel, 2006](#)), there is no evidence that RUF rebels targeted specific ethnic groups or that ethnic-misalignment between armed groups and the local population explains abuse intensity ([Bellows and Miguel, 2009](#); [Conibere et al., 2004](#); [Humphreys, 2005](#)).

The importance of diamonds (especially artisanally mined ones) has constantly decreased since the end of the civil war. The resurgence of industrial mining

operations in diamonds, bauxite, iron, and rutile has dramatically shifted the mining geography and export portfolio of Sierra Leone over the last two decades. This portfolio is now dominated by bauxite and iron exports. Overall, the mining sector accounted for 65% of Sierra Leone's exports in 2018 and for a large share of its government revenues (around 10% in recent years).<sup>20</sup> Currently, most mineral production results from six industrial mining sites, with two gold mines being planned but not yet completed. In addition, there are known deposits of other precious metals, such as chromite, coltan, columbite, limonite, platinum, tantalite, and zircon.<sup>21</sup>

### 3.2 Data

The main reason for focusing on Sierra Leone is that we can obtain granular, i.e., spatially disaggregated, data on the distribution of ethnic groups, the location and size of mines, and conflict events. Another advantage, which we leverage below, is that different minerals are mined in different parts of Sierra Leone and that the relative importance of these minerals has changed multiple times over the last two decades.

We construct a panel dataset with 107 Sierra Leonean (electoral) wards as the cross-sectional dimension and 22 years as the temporal dimension. Most wards coincide with historical chiefdoms, which are the local government units involved in selling public land to develop mines, or encompass multiple smaller chiefdoms. Wards are the lowest level of spatial aggregation for which we can obtain census information on the population shares of the different ethnic groups.<sup>22</sup> The average ward has an area of 670 km<sup>2</sup> (which is less than a quarter of the area of the 0.5 × 0.5 decimal degree grid cells commonly used in conflict studies). Our sample period starts in 1997 (as the conflict data is unavailable for earlier years) and ends in 2018 (as we have no access to some of the mining data for later years).

In what follows, we first discuss the ethnicity and natural resource data that we use to compute the two theoretical concepts we aim to empirically validate: the predicted local conflict exposure and the peace deficit. We then discuss the data on conflict events that we use in these validation exercises. Summary statistics are provided in Table B.1.

<sup>20</sup>See <https://www.investinginsierraleone.com/natural-resources/>.

<sup>21</sup>See <https://www.trade.gov/country-commercial-guides/sierra-leone-mining-and-mineral-resources>.

<sup>22</sup>We use the shape file of chiefdoms provided by [Acemoglu et al. \(2014\)](#) to build a shape file representing the boundaries of the wards reported in the 2004 Population and Housing Census of Sierra Leone.

### 3.2.1 Ethnic geography and local over-representation

To compute the predicted local conflict exposure  $e_l$  and the peace deficit  $\Delta$ , we need information on the population share  $s_l^g$  of each ethnic group  $g$  in each ward  $l$ . We obtain this information from the 2004 Housing and Population Census of Sierra Leone ([IPUMS International, 2020](#)). The census provides information on the ethnic affiliation of each tenth household in Sierra Leone at the level of wards.

The four most populous groups are the Mende (with a country-level population share of 32.9 percent), the Temne (32.2 percent), the Limba (8.3 percent), and the Kono (4.5 percent).<sup>23</sup> Our sample includes eight more groups with a population share of more than one percent. We have to assume that the spatial distribution of ethnic groups remains unchanged during our sample period, as such fine-grained data on the spatial distribution of ethnic groups is unavailable for other years. This assumption, however, is appealing given our interest in how the propensity for conflict changes in response to changes in the country’s mining geography (rather than in response to changes in its ethnic geography).

The ethnic groups’ local over-representation  $s_l^g/s^g$ , i.e., the ratios of the population share of each group in each ward relative to the group’s national population share, play a key role in our theoretical model. [Figure 2](#) plots the local over-representation of the four most populous ethnic groups across wards. We see considerable spatial variation in their local over-representation. The Kono are concentrated in the east of the country, the Limba mainly in the north, the Mende in the south, and the Temne in the west and the center.<sup>24</sup>

### 3.2.2 Mines and local resource rents

To build a time-varying measure of the resource rents  $r_l$  in each ward  $l$ , we use data on the location and size of industrial mines, which we will complement with data on artisanal and small-scale mining in an important robustness test, as well as data on the importance of the corresponding minerals over time.

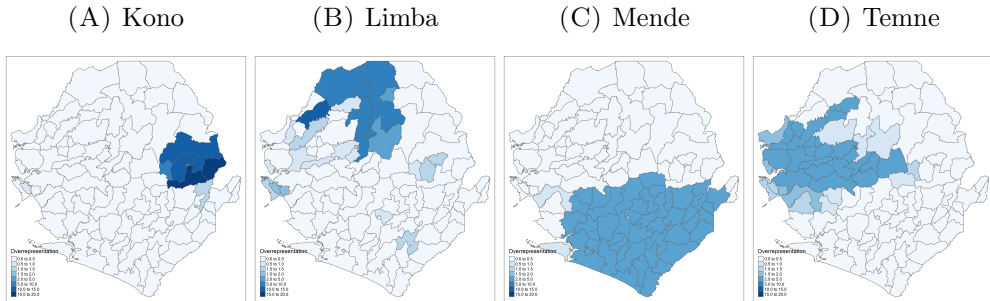
We use two spatial datasets on industrial mines. The first is the Raw Material Data (RMD) of the S&P Global Market Intelligence Unit (accessed in June 2019). The RMD provides information on global mining activities since 1980, including the (approximate) location, name, owner, primary commodity, and the

---

<sup>23</sup>These four largest ethnic groups are the only groups that are politically important throughout the sample period according to the Ethnic Power Relations data by [Wucherpfennig et al. \(2011\)](#) and [Vogt et al. \(2015\)](#).

<sup>24</sup>Figure B.1 plots the local over-representation of the remaining eight groups with a national population share of more than one percent.

FIGURE 2  
Local over-representation of the four largest ethnic groups



Notes: Panels A–D plot the local over-representation ( $s_l^g/s^g$ ) across wards for the most populous ethnic groups.

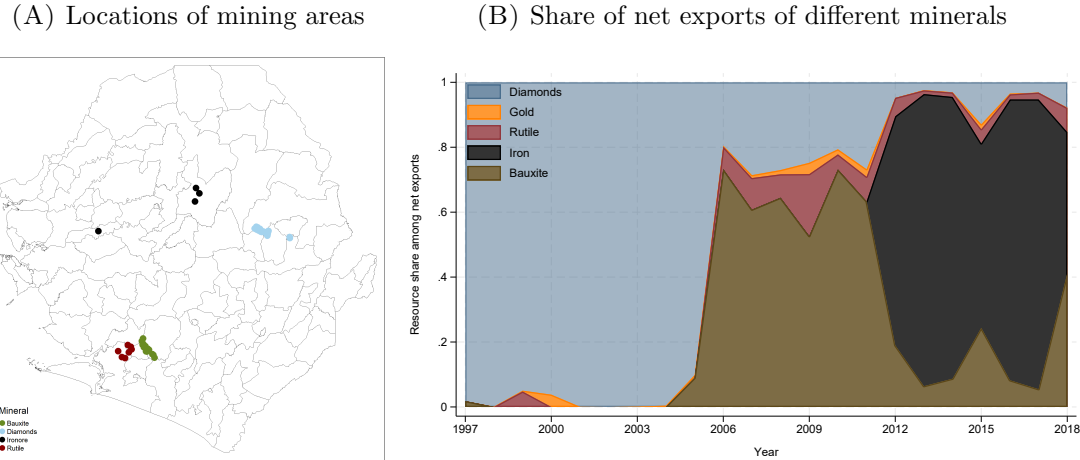
years in which a mine is active. It lacks discovery dates, and its information on the amounts extracted is incomplete. The second dataset is the global dataset of mining areas produced by [Maus et al. \(2020\)](#). They leverage recent satellite images and machine learning techniques to identify the extent of actual mines within close proximity of the sometimes imprecise locations reported in the RMD. We match the two datasets so that we have information on the primary commodity of each industrial mine (from RMD) as well as the location and shapes (polygons) of the corresponding mining areas (from [Maus et al., 2020](#)).<sup>25</sup> Panel A of [Figure 3](#) shows the resulting spatial distribution of industrial mining areas, with different colors indicating different main minerals extracted. We see that diamonds are exclusively mined in the east of the country, bauxite and rutile in the south-west, and iron primarily north of the center.

We measure the (time-varying) importance of the different minerals for Sierra Leone based on their net exports. For this purpose, we use the export and import data from [United Nations Statistics Division, UN Comtrade \(2021\)](#) and compute the value of net exports in current prices for each mineral and year (thereby setting negative values to zero). Panel B of [Figure 3](#) shows each mineral's net exports as a share of the total net exports from the five main minerals.<sup>26</sup> We see sizeable intertemporal variation in the different minerals' relative importance: Diamonds were the most important mineral up to 2004, bauxite from 2005–2011, and iron

<sup>25</sup>Some mines consist of multiple mining areas in close proximity to one another. We verify the existence of each individual industrial mine using Google Earth and auxiliary data (see Appendix A).

<sup>26</sup>Figure B.2 presents each mineral's net exports in USD as well as relative to GDP. This figure highlights that the overall importance of the mining sector has been greatest during the civil war (given the imploding GDP) and in later years (thanks to the iron boom and in spite of robust growth).

FIGURE 3  
Mining locations and the relative importance of different minerals



Notes: Panel A plots the locations of all industrial mining areas reported in [Maus et al. \(2020\)](#), with different colors indicating different minerals. Panel B plots the net exports from each mineral as a share of the total net exports from the five main minerals (bauxite, diamonds, gold, iron, rutile).

thereafter. Gold and rutile play only a minor role throughout the sample period.

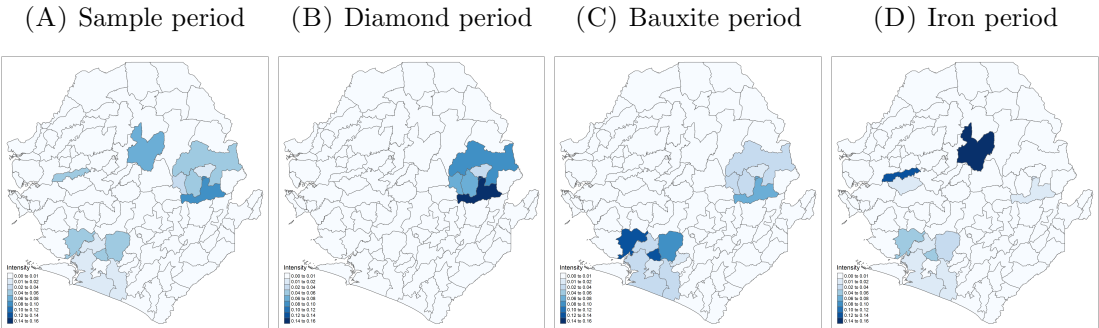
We use these data to build a measure of local resource rents  $r_l$  that increases in the size and proximity of mining areas as well as the revenues from the corresponding mineral in a given year. These assumptions are consistent with the presence of spatial spillovers from resource extraction.<sup>27</sup> We proceed in two steps. First, we distribute the annual revenues (as measured by net exports) across mining areas. For each mineral, we distribute the mineral-specific annual revenues across all mining areas that primarily extract the respective mineral; and we do so in proportion to the size of these mining areas. Second, we compute each ward's annual resource rents  $r_l$  based on the mining area-specific annual revenues. For each mining area, we assume that the rents that accrue in different wards are proportional to the inverse geodesic distance between the centroids of the mining area and these wards. The use of the inverse distance represents a specific spatial decay function. We will test for the robustness of our results with respect to alternative distance decays.

It is the relative local resource rents  $r_l/r$  that matter for local conflict exposure according to our theoretical model.<sup>28</sup> Panel A of [Figure 4](#) shows the distribution

<sup>27</sup>[Aragón and Rud \(2013\)](#) document that spillovers from gold mining can extend up to 100 km. In addition, nearby localities may also lay claims on royalties because they may host crucial infrastructure or may suffer from pollution associated with resource extraction (see, e.g., [Aragón and Rud, 2016](#); [Brueckner and Hodler, 2019](#)).

<sup>28</sup>The use of revenue shares has the added advantage that the results would remain un-

FIGURE 4  
Local resource rents averaged across different time periods



Notes: All panels plot time-averaged values of the relative local resource rents  $r_l/r$ . Panel A is based on the entire sample period (1997–2018), panel B on the period dominated by diamond exports (1997–2004), panel C on the period dominated by bauxite exports (2005–2011), and panel D on the period dominated by iron exports (2012–2018).

of  $r_l/r$ , averaged over the entire sample period, across wards. By construction, these shares are highest close to large mining areas and much smaller further away. Panels B–D show the corresponding distributions when averaging  $r_l/r$  over various shorter time periods. There are remarkable changes in the spatial patterns over time because different minerals are extracted in different parts of the country (seen in panel A of Figure 3) and important in different years (seen in panel B of Figure 3). For example, there is a large iron mine but no other mines north of the center. Therefore, this area had low relative local resource rents until the beginning of the iron boom in 2012.

### 3.2.3 Conflict

We base our measures of actual conflict on the Armed Conflict Location and Event Data (ACLED, [Raleigh et al., 2020](#)). ACLED contains information on the date and type of conflict events, the involved actors (e.g., the government, rebel groups, or civilians), and the geolocation. Following [Eberle et al. \(2020\)](#), we include events classified as battles, riots, or violence against civilians. Our results are robust to including all events (i.e., to adding protests and strategic deployments) as in [Berman et al. \(2017\)](#) and [McGuirk and Nunn \(2024\)](#) as well as to excluding individual event types (e.g., violence against civilians).

We assume that observed local conflict exposure increases in the proximity to conflict events, not least because people know that there is some randomness in the

---

changed if a fraction of the mining revenues were captured by actors outside of the model, e.g., international mining companies, as long as this fraction was identical across locations.

exact location of such events. Therefore, to construct our ward-level measure of observed local conflict exposure, we first weigh each event by the inverse distance between the conflict location and the ward’s centroid and then calculate the sum of these inverse distance-weighted events. The resulting measure of observed local conflict exposure is strictly positive (albeit potentially very close to zero) whenever there is at least one conflict event in a given year (which holds true in any year of our sample period). as conflict events occurred in all years of our sample period. This, in turn, will allow us to estimate elasticities using log-log specifications without adding an arbitrary constant (Chen and Roth, 2024). As we use the same spatial decay function in the construction of local resource rents and observed local conflict exposure, we will present robustness tests in which we change the employed decay functions for the two variables separately in order to break any potential common spatial dependence. We find no evidence that our results are driven by some unobserved spatial dependence introduced by a common decay function.

We measure the country’s aggregate propensity for conflict in a given year by the number of wards that experience at least one conflict event.

## 4 Empirical validation

In this section, we provide empirical support for our theoretically derived measures of the local and the aggregate propensity for conflict: the predicted local conflict exposure and the national peace deficit.

### 4.1 Local conflict exposure

We first compute the predicted local conflict exposure for every ward and year in our sample. Given that our theoretical model is static, we then compare the predicted and the observed local conflict exposure across wards. We later employ standard two-way fixed effects regressions as well as two-stage least squares regressions to minimize the chance that our validation is driven by unobserved factors across wards.

#### 4.1.1 Computation and graphical evidence

The predicted local conflict exposure  $e_l$  depends on the relative local resource rents  $r_l/r$  and the ethnic diversity among discordant groups  $D_{l,G^*}$  (see Section 2.3). We start the computation of the predicted local conflict exposure by determining

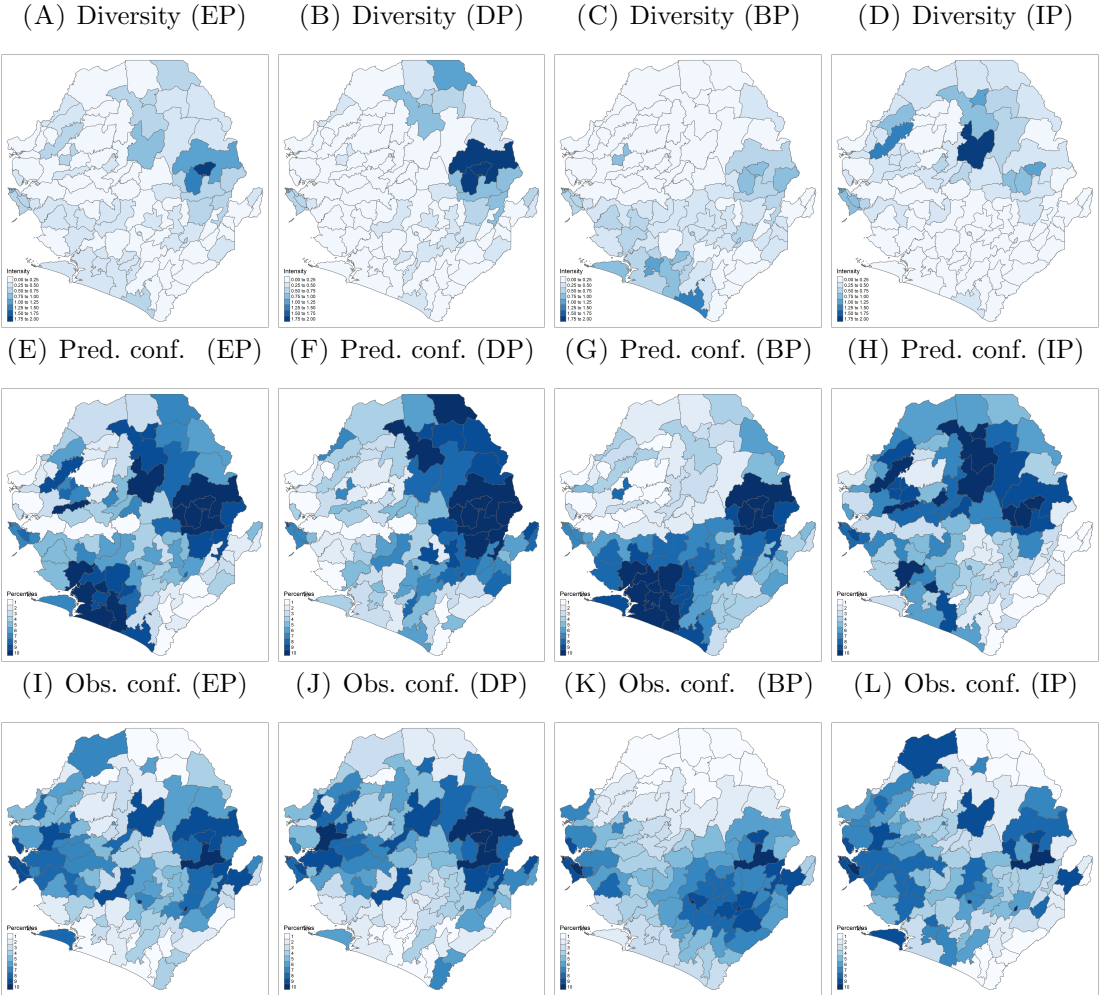
the set of discordant groups  $G^*$  in any given year (see panel A of Figure B.3). To provide some intuition on how this set depends on the country's ethnic and mining geographies, let us focus on the four main ethnic groups. The Kono are over-represented in the diamond-mining area. According to our theoretical model, they were deprived of some local resource rents and part of the set of discordant groups in most years (except in some late years when diamonds played a minor role). The Mende, who are over-represented in the bauxite-mining area, were a discordant group exclusively during the bauxite boom, and the Limba, who are over-represented in the iron-mining area, were a discordant group exclusively during the iron boom. The Temne, too, were a discordant group in some years during the iron boom.

In a second step, we use the set of discordant groups  $G^*$  and their local over-representation  $s_l/s$  to compute the ethnic diversity among discordant groups  $D_{l,G^*}$  for any ward and year. [Figure 5](#) maps these local diversity indices averaged over the entire sample period in panel A and averaged over the diamond-, bauxite- or iron-dominated periods in panels B–D. We see large changes in the ethnic diversity among discordant groups over time, resulting from the changes in the relative local resource rents and the associated changes in the set of discordant groups.

In a third step, the relative local resource rents  $r_l/r$  and the ethnic diversity among discordant groups jointly determine the predicted local conflict exposure  $e_l$  across wards. [Figure 5](#) maps the predicted local conflict exposure (in percentiles) averaged over the entire sample period in panel E and averaged over the different sub-periods in panels F–H. In every period, the predicted local conflict exposure is particularly high in areas where both the relative local resource rents and the local diversity among discordant groups are comparatively high.

Finally, we can compare the predicted and the observed local conflict exposure. [Figure 5](#) maps the observed local conflict exposure (in percentiles) averaged over the entire sample period in panel I and averaged over the different sub-periods in panels J–L. Comparing panels E and I suggests a positive correlation between predicted and observed local conflict exposures during our entire sample period. The raw correlation between the log-transformed predicted and observed local conflict exposures is 0.23. It is reassuring to see that the predicted and the observed local conflict exposure remain somewhat synchronized over time, with the raw correlation ranging from 0.22 (in the diamond-dominated period, DP) to 0.29 (in the iron-dominated period, IP).

FIGURE 5  
Visual evidence



Notes: Panels A–D plot the time-averaged ethnic diversity among discordant groups  $D_{l',G*}$ ; panels E–H the time-averaged predicted local conflict exposure  $e_l$  (in percentiles); and panels I–L the time-averaged observed local conflict exposure (in percentiles). Panels A, E, and I are based on the entire sample period (EP, 1997–2018); panels B, F, and J on the period dominated by diamond exports (DP, 1997–2004); panels C, G, and K on the period dominated by bauxite exports (BP, 2005–2011); and panels D, H and L on the period dominated by iron exports (IP, 2012–2018).

#### 4.1.2 Cross-sectional evidence

We now evaluate the predictive power of our theoretical model using the following cross-sectional OLS regression in our sample of 107 wards:

$$\ln(\text{Observed conflict exposure}_l) = \beta \ln(\text{Predicted conflict exposure}_l) + \Gamma \mathbf{X}_l + \epsilon_l, \quad (7)$$

where  $\mathbf{X}_l$  is a vector of ward-level control variables that includes the log of population based on the 2004 census and the log of area, which jointly imply that we also control for the log of population density, as well as fixed effects for the four provinces. Coefficient  $\beta$  corresponds to the elasticity of observed local conflict exposure with respect to predicted local conflict exposure. When interpreting this elasticity, it is important to keep in mind that the theoretically predicted local conflict exposure  $e_l$  only captures the systemic effect of a country's ethnic and mining geographies on the probability of local conflict and, thereby, ignores mechanical determinants like population size and political economy determinants related to, e.g., ethno-regional favoritism (as discussed in [Section 2.3](#)). While our theoretical model is silent about the magnitude of this elasticity, we expect it to be positive and statistically significant.

[Table 1](#) presents our main cross-sectional estimates with spatially clustered Conley standard errors.<sup>29</sup> Panel A shows the results when all variables are time-averaged over the entire sample period. The different columns differ in the set of control variables and fixed effects. The estimated elasticity is positive in all columns and statistically significant at the 5 percent level unless we add province-fixed effects. The estimated elasticity is 14 percent in the absence of any control variables in column (1) and drops to around 5.5 percent in the more demanding specifications in columns (3) and (4). The  $R^2$  is 0.065 in column (1) and increases to 0.245 when controlling for the ward-level population in column (2).<sup>30</sup> Hence, the systemic component highlighted by our model can explain roughly one third of the variation explained by population size, which is a well-established and rather mechanical predictor of conflict.

In panels B–D, we document a positive and statistically significant elasticity of observed local conflict exposure with respect to predicted local conflict exposure in the three time periods dominated by different minerals and, thus, different mining regions (except in column (4) of panel C). In addition, the  $R^2$  is typically of similar size as in panel A. We conclude that the results reported in panel A are not driven by a single period.

---

<sup>29</sup>Standard errors are estimated using the acreg package by [Colella et al. \(2023\)](#). We enforce a linear decay in the spatial dependence of the error terms with a distance cutoff of 100km. We later show that the results do not depend on this specific distance cutoff.

<sup>30</sup>The  $R^2$  is 0.198 when regressing the log of observed conflict exposure on the log of ward population only (result not reported).

TABLE 1  
Cross-sectional relation between predicted and observed conflict exposure

	<i>Dependent variable: Log observed conflict exposure</i>			
	(1)	(2)	(3)	(4)
<i>Panel A: Full period</i>				
Log predicted conflict exposure	0.140 (0.044)	0.120 (0.041)	0.055 (0.024)	0.053 (0.028)
R2	0.0648	0.245	0.773	0.833
<i>Panel B: Diamond period</i>				
Log predicted conflict exposure	0.097 (0.023)	0.085 (0.016)	0.068 (0.030)	0.089 (0.035)
R2	0.0967	0.238	0.537	0.684
<i>Panel C: Bauxite period</i>				
Log predicted conflict exposure	0.105 (0.048)	0.117 (0.044)	0.065 (0.027)	-0.021 (0.032)
R2	0.0649	0.245	0.736	0.794
<i>Panel D: Iron period</i>				
Log predicted conflict exposure	0.174 (0.096)	0.127 (0.074)	0.091 (0.031)	0.071 (0.028)
R2	0.0695	0.218	0.762	0.832
Population control	–	✓	✓	✓
Area control	–	–	✓	✓
Province-fixed effects	–	–	–	✓
Observations	107	107	107	107

*Notes:* The table reports the result of regressing the log of observed conflict exposure on the log of predicted conflict exposure (see [eq. 7](#)), with different control variables and fixed effects across columns (1)–(4). Population control is the log of ward population based on the 2004 census. Area control is the log of ward area. Panel A provides cross-sectional evidence after time-averaging all the included variables across the entire sample period (1997–2018). Panel B averages all variables across the period dominated by diamond exports (1997–2004), panel C across the period dominated by bauxite exports (2005–2011), and panel D by the period dominated by iron ore exports (2012–2018). Standard errors are spatially clustered with a distance cutoff of 100km.

### 4.1.3 Panel and IV evidence

The cross-sectional evidence confirms the predictive power of our theoretical model but does not lend itself to a causal interpretation due to a myriad of potentially omitted variables. To allow for causal interpretation, we use the panel of 107 wards over 22 years and run standard OLS two-way fixed effects regressions as well as two-stage least squares (2SLS) regressions with a generated instrument inspired by a commonly used instrumental variables (IV) approach.

The OLS two-way fixed effects specification is:

$$\ln(\text{Observed conflict exposure}_{lt}) = \delta \ln(\text{Predicted conflict exposure}_{lt}) + FE_l + FE_t + \varepsilon_{lt}, \quad (8)$$

where  $FE_l$  and  $FE_t$  are ward- and year-fixed effects, respectively. Our coefficient of interest is  $\delta$ , which captures the intertemporal elasticity of observed local conflict exposure with respect to predicted local conflict exposure.

OLS estimates are potentially biased because conflict events may reduce mining activities and, thereby, local resource rents and the predicted local conflict exposure. Such endogeneity concerns are common in studies on the effect of resource rents on conflict. Many researchers rely on plausibly exogenous variation in global commodity/mineral prices to mitigate these concerns (e.g., [Bazzi and Blattman, 2014](#); [Berman and Couttenier, 2015](#); [Berman et al., 2017](#); [Dube and Vargas, 2013](#)). We build on this identification strategy and construct a generated instrument for the predicted conflict exposure based on the observed group-level population shares and the relative local resource rents predicted from shift-share instruments that interact plausibly exogenous global mineral price shocks with cross-sectional exposure shares based on the wards' proximity to different mining areas. Using a generated instrument is necessary to obtain a meaningful reduced-form relationship that captures the essence of our theoretical model.

Following [Berman et al. \(2017\)](#), we measure the price shocks by the log of the global mineral prices. The mineral-specific exposure shares of a given ward are computed in a similar fashion as the local resources rents  $r_l$ . That is, we take the inverse distance to each mineral location, where each location is weighted by the time-invariant size of the corresponding mining area, and then normalize the resulting ward-level proximity values to shares. We use mineral-specific proximity-price interaction terms in the zero (or instrument generating) stage to predict the

relative local resource rents:

$$r_l/r = \sum_{j \in \{B, D, I\}} \gamma_j [\ln(\text{proximity}_l^j) \times \ln(\text{price}_t^j)] + FE_l + FE_t + \zeta_{lt}, \quad (9)$$

where  $B$ ,  $D$ , and  $I$  stand for the three main minerals: bauxite, diamonds, and iron.<sup>31</sup> These interaction terms allow for identification via exogenous shocks as in [Borusyak et al. \(2022\)](#). Our identification strategy relies on the assumption that conflict events in Sierra Leone do not impact global mineral prices. This assumption seems plausible given that Sierra Leone's exports are unimportant in these minerals' global trade, with global export shares below two percent for bauxite, diamonds, and iron ([United Nations Statistics Division, UN Comtrade, 2021](#)).

We then compute our generated instrument, which we call generated conflict exposure, using equations (3) and (5), the observed group-level population shares  $s_l^g$  and the predicted relative local resource rents  $r_l/r$ .<sup>32</sup> We use this generated instrument in the first stage of our main 2SLS specification:

$$\ln(\text{Predicted conflict exposure}_{lt}) = \psi \ln(\text{Generated conflict exposure}_{lt}) + FE_l + FE_t + \nu_{lt}. \quad (10)$$

[Wooldridge \(2010\)](#) highlights that generated instruments behave like regular instruments in models which are linear in parameters (such as 2SLS).<sup>33</sup> The second stage of our main 2SLS specification is identical to equation (8) except that we replace the explanatory variable with its predicted value.

[Table 2](#) presents our panel data estimates. Panel A reports the OLS two-way fixed effects estimates. Column (1) presents the results of equation (8). We find an estimated intertemporal elasticity of observed local conflict exposure with respect to predicted local conflict exposure of around 6 percent. Columns (2)–(4) add linear time trends for ever smaller subnational administrative units. The coefficient

---

<sup>31</sup>Net export revenues from gold and rutile are much smaller than those from the three main minerals (see [Figure 3](#)). We abstract from gold, as it is currently only mined in artisanal mines, and from rutile, as we only observe exports and prices for titanium metals (which include rutile), but not for rutile specifically. Results are nevertheless similar when adding titanium proximity-price interactions in the zero stage. (Results available upon request.) [Figure B.4](#) shows the cross-sectional and temporal distributions of the different components of our shift-share instruments used in the zero stage. The variables entering the interaction terms are all absorbed by the ward- and year-fixed effects.

<sup>32</sup>Panel B of [Figure B.3](#) shows the set of discordant groups based on the predicted relative local resource rents.

<sup>33</sup>Further adjustment of the standard errors is thus not required (see [Wooldridge, 2010](#), chapter 6).

TABLE 2  
Within-ward relation between predicted and observed conflict exposure

	<i>Dependent variable:</i>			
	<i>Log observed conflict exposure</i>			
	(1)	(2)	(3)	(4)
<i>Panel A: OLS – Dependent variable: Log observed conflict exposure</i>				
Log predicted conflict exposure	0.064 (0.020)	0.047 (0.017)	0.041 (0.018)	0.041 (0.020)
<i>Panel B: 2SLS, second stage – Dependent variable: Log observed conflict exposure</i>				
Log predicted conflict exposure	0.164 (0.050)	0.162 (0.050)	0.172 (0.055)	0.190 (0.066)
<i>Panel C: 2SLS, first stage – Dependent variable: Log predicted conflict exposure</i>				
Log generated conflict exposure	0.941 (0.066)	0.889 (0.090)	0.839 (0.096)	0.841 (0.114)
First-stage F-stat	180.7	84.89	66.59	42.69
<i>Panel D: Zero stage – Dependent variable: Relative local resource rents</i>				
Bauxite proximity-price interaction	0.420 (0.050)			
Diamond proximity-price interaction	-0.851 (0.054)			
Iron proximity-price interaction	0.109 (0.015)			
Ward- & year fixed effects	✓	✓	✓	✓
Province trends	—	✓	—	—
District trends	—	—	✓	—
Ward trends	—	—	—	✓
Observations	2354	2354	2354	2354

Notes: The table reports the results of regressing the log of observed conflict exposure on the log of predicted conflict exposure as well as ward- and year-fixed effects (see [eq. 8](#)), with different time trends across columns (1)–(4). Panel A reports OLS fixed effects regressions, panel B second-stage 2SLS regressions, and panel C the corresponding first-stage regressions (see [eq. 10](#)). The reported first-stage F-stat is the Kleibergen-Paap rk Wald F statistic. Panel D presents the zero or instrument generating stage regressions (see [eq. 9](#)) and is estimated with a fractional response model to guarantee strictly positive predicted relative resource rents for each ward and year. The set of discordant groups over time based on the predicted relative local resource rents are depicted in panel B of Figure B.3. Standard errors are spatially clustered with a distance cutoff of 100km.

estimates remain statistically significant but become somewhat smaller.<sup>34</sup>

Panels B and C of [Table 2](#) present our 2SLS estimates, phasing in more local linear time trends throughout the columns. The second-stage results in panel B show that the estimated intertemporal elasticity of observed local conflict exposure with respect to predicted local conflict exposure is around 16–19 percent, which is substantially higher than our OLS two-way fixed effects estimates. This difference suggests that mining activities may indeed fall in response to conflict events. Panel C reports the first-stage results. The first-stage F-stats of the instruments far exceed common thresholds for instruments' power—as is common for generated instruments. Finally, panel D shows that our price proximity interactions have predictive power for the relative local resource rents.<sup>35</sup>

#### 4.1.4 Sensitivity analysis and external validity

We conduct various robustness tests. First, we focus on the coding of our dependent variable: the observed local conflict exposure. We start by including all ACLED events to construct our dependent variable (as in, e.g., [Berman et al., 2017](#); [McGuirk and Nunn, 2024](#)), after which we drop single event categories and actor types in turn. The coefficient estimates remain similar throughout most of these perturbations (see Figure B.5). The main exception is that the coefficient estimates (especially the 2SLS estimates) become considerably smaller if we exclude conflict events involving rebels and militias. This finding is reassuring as it is exactly those actors that we expect to engage in local conflicts according to our theoretical argument.

Second, we focus on the construction of our independent variable, the predicted conflict exposure. First, we include artisanal and small-scale mining fields and distribute the mineral-specific export revenues across all industrial and artisanal mines when computing local resource rents (see Appendix A for details). Second, we distribute the (industrial) resource revenues across mines in proportion to the

---

<sup>34</sup>A potential issue is that the two-way fixed effect estimator introduces a correlation between the regression weights and treatment intensity, thus biasing our estimates ([De Chaisemartin and d'Haultfoeuille, 2020](#)). However, testing for the correlation between weights and treatment intensity suggests that our estimator does not suffer from the issue in columns (1) and (2), but that including more restrictive time trends leads to a correlation. Given the similarity in the estimates across columns, we view this as a minor issue in our setting.

<sup>35</sup>Panel D shows that increases in bauxite and, to a lesser extent, iron prices have strong positive effects on the predicted relative local resource rents in wards close to bauxite and iron mines. We also see that increases in diamond prices reduce predicted local resource rents in wards in close proximity to diamond mines. The main reason for this (maybe surprising) result is that the rise in diamond prices coincided with the decreasing importance of the diamond sector in Sierra Leone after the civil war.

nighttime light emissions within the mining areas rather than in proportion to the size of these areas when computing local resource rents. Third, we recompute the ethnic diversity among discordant groups based on the population distribution among the four largest groups, which are the only groups that were politically relevant throughout the sample period (according to [Wucherpfennig et al., 2011](#)). Our results remain similar throughout these perturbations (see Figure B.6).

Third, we test whether our results are driven by the spatial decay function,  $distance^{-1}$ , that we use to compute the local resource rents and the observed local conflict exposure.<sup>36</sup> However, we find similar results for a range of distance decays from  $distance^{-0.5}$  to  $distance^{-2}$ . Importantly, we also find similar results when varying the distance decay only for the measurement of either local resource rents or observed local conflict exposure in order to break any potential spatial correlation stemming from a common decay function (see Figure B.7). Relatedly, the precision of our estimates does not depend on the specific distance cutoff that we employ in the calculation of the Conley standard errors (see Figure B.8).

Fourth, we test whether the effect of the predicted local conflict exposure simply reflects the effect of local resource rents. For this purpose, we control for the log of (absolute) local resource rents  $r_l$ , the relative local resource rents  $r_l/r$ , and the interaction of an indicator variable for the presence of a mine and the log of the global price of the main mineral extracted in this ward (which is the proxy for mining in [Berman et al., 2017](#)). The effect of predicted local conflict exposure on observed local conflict exposure remains statistically significant and of similar magnitude in most specifications (see Figure B.9). In contrast, the effects of these local resource measures are typically statistically insignificant or negative. These results underline the importance of the systemic conflict pressure that results from the interplay between the country's ethnic geography and its mining geography.

Fifth, we control for the share of the population in a ward that identifies with the same ethnic group as the current president of Sierra Leone. This exercise is inspired by our theoretical model, in which the planner may have ward-specific priority weights (see equation (1)), and the literature on ethno-regional favoritism. We also control for the population share identifying with politically included ethnic groups (according to [Wucherpfennig et al., 2011](#)). We find virtually unchanged elasticity estimates (see Figure B.9), suggesting that ethno-regional favoritism does not substantially alter the systemic conflict pressure captured by our variable of interest.

---

<sup>36</sup>The natural resource literature and the conflict literature, unlike the trade literature, lack well-established distance decay functions.

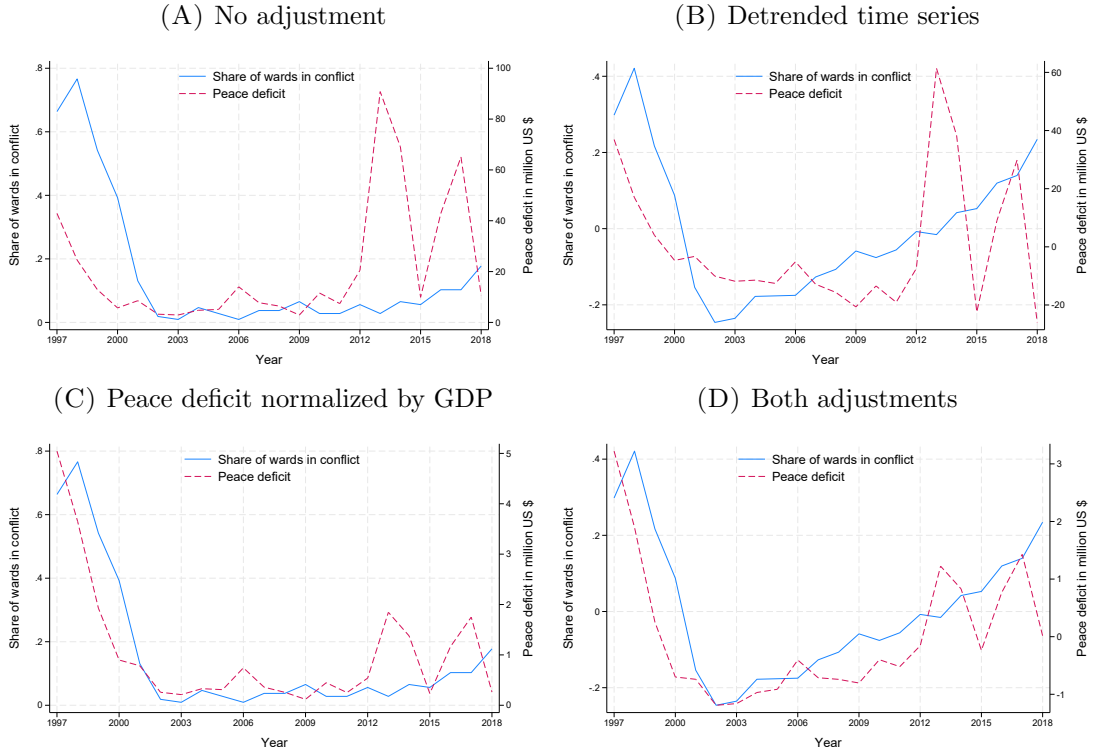
Finally, we assemble a second dataset to test the external validity of our main cross-sectional results. For that purpose, we prepare data at the level of  $0.5 \times 0.5$  decimal degree grid cells across eight West African countries. To overcome the lack of high-quality data on the spatial distribution of ethnic groups, we combine the Spatially Interpolated Data on Ethnicity by [Müller-Crepon and Hunziker \(2018\)](#) with geospatial population estimates. We find that results are very similar when restricting our attention to the (only) 39 grid cells in Sierra Leone. The estimated elasticities become somewhat smaller but remain positive and statistically significant in the full sample of all these eight countries. We discuss this second dataset and our results in detail in Appendix C.

## 4.2 Changes in country-wide conflict over time

We now analyze whether our theoretical model is also suited to predict intertemporal changes in a country's aggregate propensity for conflict. We have argued earlier that the national peace deficit  $\Delta$ , which quantifies the extra transfers necessary to guarantee peace in every location, is a good theoretical proxy for this propensity. In practice, however, additional fiscal capacity for peacekeeping can be generated by taxing other sectors of the economy or by borrowing, and such fiscal capacity is arguably proportional to the size of the economy. This capacity was low in the years of the civil war (which ended in 2002) and was increasing thereafter in accordance with the growing size of the economy. We, therefore, propose to detrend the two time series (i.e., actual and predicted aggregate propensity for conflict) or to compute the peace deficit in percent of GDP.

[Figure 6](#) plots the time series for actual and predicted aggregate propensity for conflict, where the former corresponds to the share of wards that experience at least one conflict event in a given year (see [Section 3.2.3](#)). The time series are detrended in panels B and D, and the peace deficit is normalized by GDP in panels C and D. We see that the two variables co-move quite strongly as soon as we use at least one of the two proposed approaches to account for the large changes in the size of the economy and the state's fiscal capacity over time. The raw correlation between the two time series is 0.076 in panel A but increases to 0.399, 0.824, and 0.795 in panels B, C, and D, respectively. We conclude that our theoretical model also has considerable predictive power when it comes to explaining intertemporal changes in a country's aggregate propensity for conflict.

FIGURE 6  
Changes in country-wide propensity for conflict over time



Notes: Panel A plots the share of wards with at least one conflict event (blue line) and the peace deficit  $D$  in million US dollars (dashed red line) over time. Panel B replicates panel A after detrending both time series. Panel C replicates panel A after dividing the peace deficit by GDP. Panel D replicates panel A after dividing the peace deficit by GDP and then detrending both time series.

## 5 Counterfactual analyses

We now employ our two theoretical concepts – the peace deficit and local conflict exposure – to predict how the hypothetical development of known mineral deposits in Sierra Leone would shape conflict in the country. We do so for all discovered mineral deposits reported by the RMD as of 2019 (listed in Table A.1). Panel A of Figure 7 shows that these deposits differ with respect to their locations and main minerals (using differently colored symbols for the different minerals). For some of these deposits, we know the holder of the prospecting license, but we lack information on the current development plans. For others, the government has already awarded mining licenses. Examples include the Baomahun project, whose license holder is FG Gold, and the Nimini–Komahun project, whose license holder is Nimini Holdings Limited.

In our framework, opening new mines corresponds to changing the spatial

distribution of local resource rents. We base our counterfactual analyses on the following scenario: First, the revenues generated by the six existing industrial mines are the same as they were in the last year of our sample period. Second, new mines generate 10 percent of the aggregated revenues generated by the six existing industrial mines combined.<sup>37</sup>

## 5.1 New mines and the aggregate propensity for conflict

We use the peace deficit to predict the effects of new mines and the corresponding change in the spatial distribution of local resource rents on the aggregate propensity for conflict. The peace deficit quantifies the extra transfers necessary to guarantee peace both at the national level and in every ward. Recall that the peace deficit can be written as  $\Delta(\mathbf{r}, \mathbf{s}, G^*) = \sum_{g \in G^*} (\sum_{l \in L} r_l s_l^g - rs^g)$ . Hence, it depends on the distributions of resource rents and discordant groups across wards. Any change in the peace deficit caused by the development of a new mine can thus be decomposed into a direct and an indirect effect.

The direct effect is the change in the peace deficit that the shift in the resource rent distribution  $\mathbf{r}$  would cause if the set of discordant groups  $G^*$  remained fixed. It captures the extent to which the new mine raises the propensity for conflict by shifting resource rents to wards where discordant groups are over-represented. The indirect effect is the change in the peace deficit resulting from the revision of the set of discordant groups  $G^*$  (if any) caused by the development of the new mine, evaluated at the new distribution of local resource rents. The indirect effect is driven by groups becoming discordant (typically groups over-represented around new mines) and groups leaving the set of discordant groups (typically groups under-represented around new mines).<sup>38</sup>

Panel B of Figure 7 reports the predicted changes in the peace deficit from each hypothetical mining project. The direct and indirect effects are shown using red and white bars, respectively. We see that the development of many deposits, including the Baomahun and the Nimini-Komahun projects, are predicted to increase the peace deficit and, therefore, the aggregate propensity for conflict. However, a considerable share of potential mines, including two potential gold

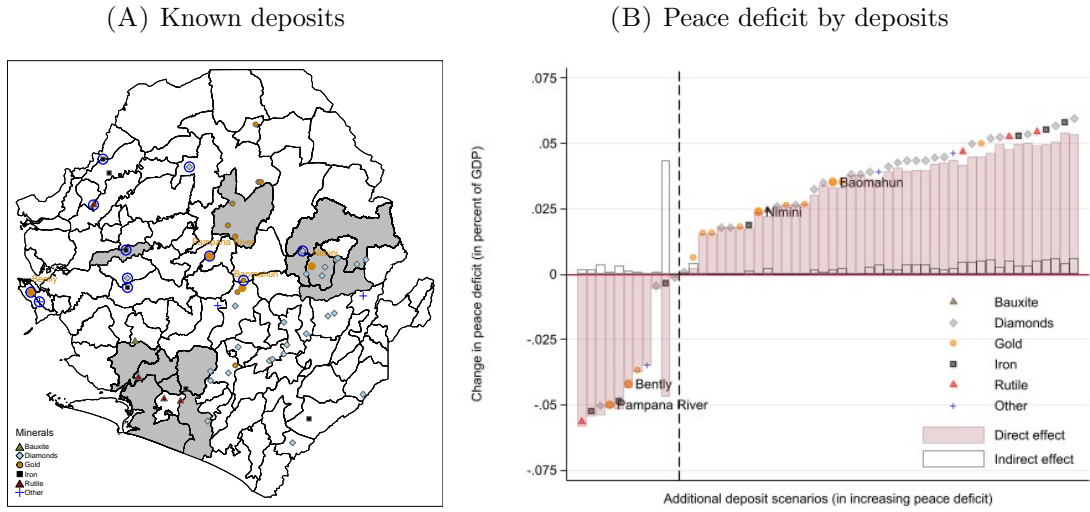
---

<sup>37</sup>The capacities of new mining projects are unknown. It is straightforward to run the counterfactual analyses with different assumptions about the revenues generated by new and existing mines.

<sup>38</sup>To define the direct and the indirect effect more explicitly, let us write the set of discordant groups as  $G^*(\mathbf{r}, \mathbf{s})$ , and let  $\mathbf{r}$  and  $\hat{\mathbf{r}}$  be the resource rent distributions before and after the mine opening. Then, the direct effect is  $\Delta(\hat{\mathbf{r}}, \mathbf{s}, G^*(\mathbf{r}, \mathbf{s})) - \Delta(\mathbf{r}, \mathbf{s}, G^*(\mathbf{r}, \mathbf{s}))$ , and the indirect effect  $\Delta(\hat{\mathbf{r}}, \mathbf{s}, G^*(\hat{\mathbf{r}}, \mathbf{s})) - \Delta(\hat{\mathbf{r}}, \mathbf{s}, G^*(\mathbf{r}, \mathbf{s}))$ .

FIGURE 7

New mines and their predicted effects on aggregate propensity for conflict



*Notes:* Panel A depicts the locations of known mineral deposits (as of 2019 based on the RMD, excluding deposits directly located in the national or a provincial capital city). Different symbols and colors indicate the primary metals of the deposits (with Other referring to nickel and ilmenite). The locations and names of the four potential new gold mines explicitly mentioned in Section 5 are highlighted with larger dots. The wards highlighted in grey depict the locations of currently active mines (as of 2018). Blue circles indicate deposits that decrease the peace deficit based on the analysis reported in panel B. Panel B plots the simulated changes in the peace deficit (measured in percent of GDP) from mining any of the known deposits shown in Panel A under the assumption that the revenues generated at this deposit are equal to 10 percent of the revenues of all existing mines combined. Different colors and shapes represent the total effect of different minerals. The red bars represent the direct effects (keeping the set of discordant groups fixed), and the white bars represent the indirect effects due to the change in the set of discordant groups.

mines at the Bently and the Pampana River deposits, are predicted to reduce the peace deficit.<sup>39</sup> We indicate these mines with blue circles in the map in panel A of Figure 7.

The variation in the predicted total effects on the peace deficit is, to a large extent, driven by the variation in the direct effects. Given that discordant groups are by definition over-represented in resource-rich locations, the direct effect tends to be positive for new mines located close to existing mines, such as the Nimini-Komahun project close to existing diamond mines, but negative for new mines that are far from existing mines, such as the Bentley deposit close to Freetown in the far west. However, the local ethnic geography matters as well. The Baomahun project and the Pampana River deposit are relatively close to one another, but their (direct) effects on the peace deficit are very different. The reasons are that

<sup>39</sup>The Bentley deposit was prospected by Njahili Resources Limited, and the Pampana River deposit is owned by Sunergy.

the Mende are locally over-represented around the Baomahun project (and most of the peace-reducing deposits in the southeast) while the Temne are locally over-represented around the Pampana River deposit (and some of the peace-promoting deposits in the country’s northwest); and that the Mende are a discordant group while the Temne are not.

The indirect effects are either zero or small and positive. Positive indirect effects are typically driven by a single ethnic group joining or leaving the set of discordant groups. For example, the Kono (over-represented in the east) leave this set in case of new mines at the Bently or the Pampana River deposit, and the Limba (over-represented in the north) leave it in case of the Baomahun project.<sup>40</sup> We conclude that “mining for peace” by developing new deposits seems feasible in Sierra Leone, especially in the country’s northwest and far west.<sup>41</sup>

In a similar vein, the peace deficit could be used to predict how changes in the world market prices of some minerals would affect the country’s aggregate propensity for conflict. Figure B.14 shows that higher mineral prices tend to increase the peace deficit but that these effects differ across minerals.<sup>42</sup>

## 5.2 New mines and the local propensity for conflict

We now use the local conflict exposure  $e_l$ , defined in equation (5), to predict the effect of hypothetical new mines on the local propensity for conflict. This measure captures the systemic component of the local conflict pressure resulting from the interaction of the country’s ethnic and mining geographies. Again, we can distinguish between a direct effect that results from the change in the relative local resource rents  $r_l/r$  and, possibly, an indirect effect that results from changes in the set of discordant groups  $G^*$  and, therefore, the local ethnic diversity among dis-

---

<sup>40</sup>There is one outlier with a large indirect effect in panel B of Figure 7. This is the Kukuna iron mine in the north west of the country. This large indirect effect is because the Susu are heavily over-represented around this deposit and become a discordant group. In general, the indirect effects tend to become larger if the new mines generate higher revenues (as illustrated in Figure B.10).

<sup>41</sup>This insight is particularly relevant to policymakers and international mining companies if peace-promoting mines are not systematically less attractive than peace-reducing mines from an economic viewpoint. Figure B.12 provides suggestive evidence that the peace deficit of mines is not systematically correlated with observable local risk factors (proxied by conflict incidents within 50km) or trade costs (proxied by the distance to the capital city, Freetown, which hosts the only container port within the country).

<sup>42</sup>In case of bauxite, diamonds, and rutile the effects are quite large and mostly direct, because groups like the Mende and the Kono, which are over-represented in the corresponding mining areas, are discordant groups already. In contrast, the effect is smaller and mostly indirect for iron. The reason is that some groups over-represented in parts of the iron-mining areas, in particular the Temne, only become discordant when the iron price increases.

cordant groups  $D_{l,G^*}$  (evaluated at the new distribution of local resource rents).<sup>43</sup>

The direct effect of a new mine on the local conflict exposure obviously depends on the ward under consideration. The direct effect is positive for wards where the relative local resource rents increase, in particular, the ward hosting the new mine. It is negative for all the wards that experience a decrease in the relative local resource rents. The indirect effect is typically positive in the ward hosting the new mine – again, because groups over-represented around new mines are the ones typically becoming discordant, while groups under-represented around new mines may leave the set of discordant groups. The indirect effects on the local conflict exposure in other wards are ambiguous and depend on the location of the new mines and the country’s entire ethnic and mining geographies.

Panel A of [Figure 8](#) illustrates how hypothetical new mines change the local conflict exposure in the wards hosting the corresponding deposits. The direct effects are always positive but differ in their size due to differences in the local diversity among discordant groups. The indirect effects tend to be positive too. They are typically zero or small but can become large if a new mine in a resource-rich location makes a locally over-represented group join the set of discordant groups, such as in the case of two hypothetical new gold mines north of the center and close to the already active Tonkolili iron mine. It follows that the total effects on local conflict exposure in the wards hosting the new mines are always positive but vary greatly in size.

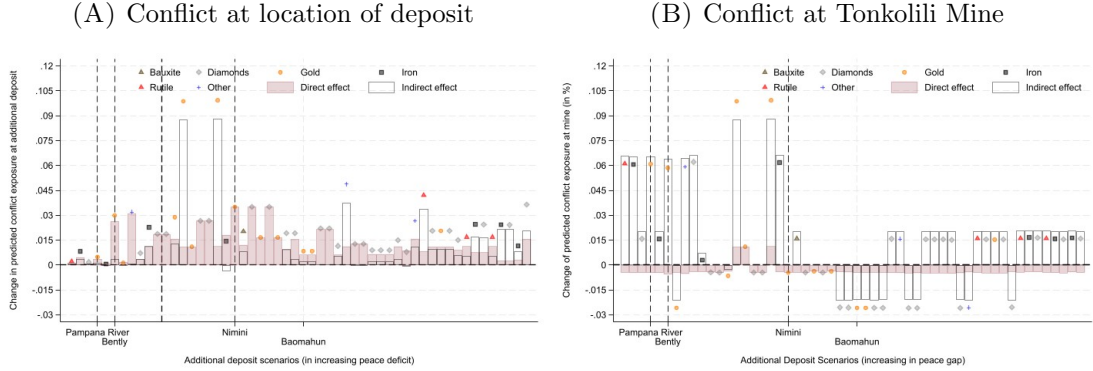
We have ordered the new mines by their effects on the peace deficit. This serves to illustrate that there is no clear relation between a new mine’s effects on the aggregate propensity for conflict and the propensity for conflict around the mine. This pattern also holds for the four hypothetical new gold mines on which we focused above. For example, while new mines at the Bently and the Pampana River deposits would both reduce the aggregate propensity for conflict, the latter would cause a substantially smaller increase in the local propensity for conflict than the former. The reason is the lower local ethnic diversity among discordant groups in the ward hosting Pampana River deposit, where all discordant groups are under-represented, than in the ward hosting the Bently deposit, where two discordant groups (the Limba and the Sherbo) are heavily over-represented. Moreover, the Baomahun project raises the aggregate propensity for conflict considerably but has only a small effect on local conflict exposure.

We can also predict the effects of new mines on local conflict exposure in wards

---

<sup>43</sup>Building on definition (5) and the notation introduced in footnote 38, the direct effect can be written as  $[(\hat{r}_l/\hat{r}) - (r_l/r)] D_{l,G^*}(\mathbf{r}, \mathbf{s})$ , and the indirect effect as  $(\hat{r}_l/\hat{r}) [D_{l,G^*}(\hat{\mathbf{r}}, \mathbf{s}) - D_{l,G^*}(\mathbf{r}, \mathbf{s})]$ .

FIGURE 8  
Predicted effects of new mines on local propensity for conflict



Notes: Panels A and B plot the change in the local conflict exposure  $e_l$  in different wards in response to the same simulated new mining activities as in Panel B of Figure 7. Panel A shows the effects on local conflict exposure in the wards where the new corresponding deposits are located, and panel B the effects on local conflict exposure in the ward where the Tonkolili mine is located. Different colors and shapes represent the total effects for different minerals. The red bars represent the direct effects (keeping the set of discordant groups fixed), and the white bars represent the indirect effects due to the change in the set of discordant groups. The newly mined deposits are ordered by their effects on the peace deficit (as shown in Panel B of Figure 7).

other than those hosting new mines. To illustrate this possibility, we predict the effects of each hypothetical new mine on the propensity for conflict in the wards hosting the six existing mines. We report the results for the large Tonkolili iron mine (located north of the center) in panel B of Figure 8 and the results for the other mines in Figure B.13. We see in panel B of Figure 8 that the direct effects are negative for most new mines, as higher resource rents elsewhere slightly reduce the relative local resource rents in the ward hosting the Tonkolili mine. Of course, the direct effect is positive in the case of new mines nearby. The indirect effects are large in absolute values (as compared to the direct effects), and they vary greatly as they depend on the country's entire ethnic and mining geographies. This is not specific to the Tonkolili mine. In general, the indirect effects tend to be larger than the direct effects for wards far away from new mining activity.

## 6 Conclusion: Mining policies for peace

Previous research suggests that natural resource rents are typically a curse for resource-extracting countries and regions. Given the increasing global demand for minerals from ethnically diverse and historically conflict-prone countries, we have reassessed the effects of mining on conflict. We have gone beyond purely local

average effects and focused on the systemic component of the local conflict risk that results from the country's entire ethnic and mining geographies. We document that the development of different mineral deposits can have very different effects on both a country's aggregate propensity for conflict as well as the spatial distribution of conflict risks. Governments, international mining companies, international organizations, and advocacy groups may benefit from taking these aggregate and local conflict externalities into account when deciding whether and under what terms certain deposits can be developed.

Governments, which may be primarily concerned with a country's aggregate propensity for conflict, should focus on the effect of potential new mining projects on the peace deficit. The change in the peace deficit resulting from a new mine corresponds to the (positive or negative) monetary transfer to the planner that would be necessary to ensure that this project leaves the country's aggregate propensity for conflict unchanged. Governments should make use of this information when designing policy. Ideally, they would include the change in the peace deficit in the price of the mining license. Alternatively, they could design the royalty and tax schemes in a manner that reflects the change in the peace deficit. If a government is unwilling or unable to implement any of these relatively subtle policies, it could take the aggregate conflict externalities into account when deciding whether to allow a new mining project in a specific location. In addition, governments may also want to act upon information about local conflict externalities captured by our measure of local conflict exposure, e.g., if they are particularly concerned by higher conflict risks in some economically or politically important locations.

Many international mining companies (IMCs) care about conflict risks as well, e.g., because conflict can increase their production and transportation costs or undermine their social license to operate, i.e., "the ongoing approval and broad acceptance of society to conduct [their] activities" ([Prno and Slocombe, 2012](#), p. 346). Hence, these IMCs would benefit from knowing the aggregate and local conflict externalities of their potential new mining projects. For example, if an IMC knew how its new project shaped the spatial distribution of local conflict risks, it would be better positioned to estimate the production costs at the mining site, the transportation costs from this site to the port, and the difficulty of getting the social license to operate.

Already today, many IMCs follow the UN Guiding Principles on Business and Human Rights, which are increasingly codified in national or supranational law. These principles require companies to conduct human rights due diligence, among others, in order to avoid harming local communities. We are not the first to argue

that human rights due diligence should take the effects on conflict and violence into account.<sup>44</sup> However, we are the first to suggest a theoretical framework that can be brought to the data and help assess aggregate and local conflict externalities of new mining projects.

---

<sup>44</sup>For example, in a [joint statement on conflict and due diligence legislation](#), many human rights experts criticize that the due diligence directive proposed by the European Commission lacks special provisions for (mining) companies active in conflict-prone areas.

## References

Acemoglu, D., T. Reed, and J. A. Robinson (2014). Chiefs: Economic development and elite control of civil society in Sierra Leone. *Journal of Political Economy* 122(2), 319–368.

Adhvaryu, A., J. Fenske, G. Khanna, and A. Nyshadham (2021). Resources, conflict, and economic development in Africa. *Journal of Development Economics* 149, 102598.

Amarasinghe, A., P. Raschky, Y. Zenou, and J. Zhou (2020). Conflicts in spatial networks. Discussion Paper 14300, Centre for Economic Policy Research.

Aragón, F. M. and J. P. Rud (2013). Natural resources and local communities: Evidence from a Peruvian gold mine. *American Economic Journal: Economic Policy* 5(2), 1–25.

Aragón, F. M. and J. P. Rud (2016). Polluting industries and agricultural productivity: Evidence from mining in Ghana. *Economic Journal* 126(597), 1980–2011.

Armand, A., A. Coutts, P. C. Vicente, and I. Vilela (2020). Does information break the political resource curse? Experimental evidence from Mozambique. *American Economic Review* 110(11), 3431–3453.

Atkin, D., E. Colson-Sihra, and M. Shayo (2021). How do we choose our identity? A revealed preference approach using food consumption. *Journal of Political Economy* 129(4), 1193–1251.

Bazzi, S. and C. Blattman (2014). Economic shocks and conflict: Evidence from commodity prices. *American Economic Journal: Macroeconomics* 6(4), 1–38.

Bellows, J. and E. Miguel (2006). War and institutions: New evidence from Sierra Leone. *American Economic Review* 96(2), 394–399.

Bellows, J. and E. Miguel (2009). War and local collective action in Sierra Leone. *Journal of Public Economics* 93(11–12), 1144–1157.

Berman, N. and M. Couttenier (2015). External shocks, internal shots: the geography of civil conflicts. *Review of Economics and Statistics* 97(4), 758–776.

Berman, N., M. Couttenier, and V. Girard (2023). Mineral resources and the salience of ethnic identities. *Economic Journal* 133(653), 1705–1737.

Berman, N., M. Couttenier, D. Rohner, and M. Thoenig (2017). This mine is mine! How minerals fuel conflicts in Africa. *American Economic Review* 107(6), 1564–1610.

Bester, H. and K. Wärneryd (2006). Conflict and the social contract. *Scandinavian*

*Journal of Economics* 108(2), 231–249.

Binzel, C., D. Fehr, and A. Link (2024). Can international initiatives promote peace? Diamond certification and armed conflicts in Africa. Discussion Paper 18450, Centre for Economic Policy Research.

Blattman, C. (2022). *Why We Fight: The Roots of War and the Paths to Peace*. Penguin Books.

Borusyak, K., P. Hull, and X. Jaravel (2022). Quasi-experimental shift-share research designs. *Review of Economic Studies* 89(1), 181–213.

Brückner, M. and A. Ciccone (2010). International commodity prices, growth and the outbreak of civil war in Sub-Saharan Africa. *Economic Journal* 120(544), 519–534.

Brüderle, A. and R. Hodler (2019). Effect of oil spills on infant mortality in Nigeria. *Proceedings of the National Academy of Sciences* 116(12), 5467–5471.

Burgess, R., R. Jedwab, E. Miguel, A. Morjaria, and G. Padró i Miquel (2015). The value of democracy: Evidence from road building in Kenya. *American Economic Review* 105(6), 1817–1851.

Chen, J. and J. Roth (2024). Logs with zeros? Some problems and solutions. *Quarterly Journal of Economics* 139(2), 891–936.

Christensen, H. B., M. Maffett, and T. Rauter (2024). Reversing the resource curse: Foreign corruption regulation and the local economic benefits of resource extraction. *American Economic Journal: Applied Economics* 16(1), 90–120.

Colella, F., R. Laliv, S. O. Sakalli, and M. Thoenig (2023). acreg: Arbitrary correlation regression. *Stata Journal* 23(1), 119–147.

Collier, P. and A. Hoeffer (2004). Greed and grievance in civil war. *Oxford Economic Papers* 56(4), 563–595.

Conibere, R., J. Asher, K. Cibelli, J. Dudukovich, R. Kaplan, and P. Ball (2004). Statistical appendix to the report of truth and reconciliation commission, report of Sierra Leone. *Human Rights Data Analysis Group, The Benetech Initiative* 134.

Corvalan, A. and M. Vargas (2015). Segregation and conflict: An empirical analysis. *Journal of Development Economics* 116, 212–222.

De Chaisemartin, C. and X. d'Haultfoeuille (2020). Two-way fixed effects estimators with heterogeneous treatment effects. *American Economic Review* 110(9), 2964–2996.

De Luca, G., R. Hodler, P. A. Raschky, and M. Valsecchi (2018). Ethnic favoritism: An axiom of politics? *Journal of Development Economics* 132, 115–129.

Desmet, K., I. Ortúñoz-Ortín, and R. Wacziarg (2012). The political economy of linguistic cleavages. *Journal of Development Economics* 97(2), 322–338.

Desmet, K., I. Ortúñoz-Ortín, and R. Wacziarg (2017). Culture, ethnicity, and diversity. *American Economic Review* 107(9), 2479–2513.

Dube, O. and J. F. Vargas (2013). Commodity price shocks and civil conflict: Evidence from Colombia. *Review of Economics and Statistics* 80(4), 1384–1421.

Eberle, U. J., D. Rohner, and M. Thoenig (2020). Heat and hate: Climate security and farmer-herder conflicts in Africa. Discussion Paper 15542, Centre for Economic Policy Research.

Esteban, J., L. Mayoral, and D. Ray (2012). Ethnicity and conflict: An empirical study. *American Economic Review* 102(4), 1310–1342.

Esteban, J., M. Morelli, and D. Rohner (2015). Strategic mass killings. *Journal of Political Economy* 123(5), 1087–1132.

Esteban, J. and D. Ray (2008). On the salience of ethnic conflict. *American Economic Review* 98(5), 2185–2202.

Fearon, J. D. (1995). Rationalist explanations for war. *International Organization* 49(3), 379–414.

Fey, M. and K. W. Ramsay (2009). Mechanism design goes to war: Peaceful outcomes with interdependent and correlated types. *Review of Economic Design* 13(3), 233–250.

Gehring, K., S. Langlotz, and K. Stefan (2023). Stimulant or depressant? Resource-related income shocks and conflict. *Review of Economics and Statistics* forthcoming.

Hodler, R., M. Lechner, and P. Raschky (2023). Institutions and the resource curse: new insights from causal machine learning. *PLOS One* 18(6), e0284968.

Hodler, R. and P. A. Raschky (2014). Regional favoritism. *Quarterly Journal of Economics* 129(2), 995–1033.

Hörner, J., M. Morelli, and F. Squintani (2015). Mediation and peace. *Review of Economic Studies* 82(4), 1483–1501.

Humphreys, M. (2005). Natural resources, conflict, and conflict resolution: Uncovering the mechanisms. *Journal of Conflict Resolution* 49(4), 508–537.

IPUMS International (2020). Minnesota Population Center. Integrated Public Use Microdata Series, International: Version 7.3 2004 Population and Housing Census. Available at <https://doi.org/10.18128/D020.V7.3>.

Jackson, M. O. and M. Morelli (2007). Political bias and war. *American Economic Review* 97(4), 1353–1373.

Jackson, M. O. and M. Morelli (2011). The reasons for wars: An updated survey. In *The Handbook on the Political Economy of War*, Chapter 3. Edward Elgar Publishing.

Kaldor, M. and J. Vincent (2006). Evaluation UNDP assistance to conflict-affected countries: Case study Sierra Leone. Technical report, United Nations Development Programme Evaluation Office.

Kandeh, J. D. (1992). Politicization of ethnic identities in Sierra Leone. *African Studies Review* 35(1), 81–99.

König, M. D., D. Rohner, M. Thoenig, and F. Zilibotti (2017). Networks in conflict: Theory and evidence from the great war of Africa. *Econometrica* 85(4), 1093–1132.

Laurent-Lucchetti, J., D. Rohner, and M. Thoenig (2024). Ethnic conflict and the informational dividend of democracy. *Journal of the European Economic Association* 22(1), 73–116.

Lei, Y.-H. and G. Michaels (2014). Do giant oilfield discoveries fuel internal armed conflicts? *Journal of Development Economics* 110, 139–157.

Matuszeski, J. and F. Schneider (2006). Patterns of ethnic group segregation and civil conflict. Working paper, Center for Global Development.

Maus, V., S. Giljum, J. Gutschlhofer, D. M. da Silva, M. Probst, S. L. Gass, S. Luckeneder, M. Lieber, and I. McCallum (2020). A global-scale data set of mining areas. *Scientific Data* 7(1), 1–13.

McGuirk, E. F. and N. Nunn (2024). Transhumant pastoralism, climate change and conflict in Africa. *Review of Economic Studies* forthcoming.

Montalvo, J. G. and M. Reynal-Querol (2005). Ethnic polarization, potential conflict, and civil wars. *American Economic Review* 95(3), 796–816.

Morelli, M., L. Ogliari, and L. Hong (2024). Power mismatch and civil conflict: An empirical investigation. *Economic Policy* 39(117), 45–105.

Morelli, M. and D. Rohner (2015). Resource concentration and civil wars. *Journal of Development Economics* 117, 32–47.

Müller-Crepon, C. and P. Hunziker (2018). New spatial data on ethnicity: Introducing SIDE. *Journal of Peace Research* 55(5), 687–698.

Novta, N. (2016). Ethnic diversity and the spread of civil war. *Journal of the European Economic Association* 14(5), 1074–1100.

Prno, J. and D. S. Slocombe (2012). Exploring the origins of ‘social license to operate’ in the mining sector: Perspectives from governance and sustainability theories. *Resources Policy* 37(3), 346–357.

Raleigh, C., A. Linke, and C. Dowd (2020). Armed Conflict Location and Event Dataset (ACLED). *Codebook Version 2*.

Ray, D. (2009). Costly conflict under complete information. Technical report, New York University.

Roth, A. E. (2002). The economist as engineer: Game theory, experimentation, and computation as tools for design economics. *Econometrica* 70(4), 1341–1378.

Spolaore, E. and R. Wacziarg (2016). War and relatedness. *Review of Economics and Statistics* 98(5), 925–939.

United Nations Statistics Division, UN Comtrade (2021). International Merchandise Trade Statistics. Available at: <http://comtrade.un.org/>.

Vogt, M., N.-C. Bormann, S. Rüegger, L.-E. Cederman, P. Hunziker, and L. Girardin (2015). Integrating data on ethnicity, geography, and conflict: The ethnic power relations data set family. *Journal of Conflict Resolution* 59(7), 1327–1342.

Wooldridge, J. M. (2010). *Econometric Analysis of Cross Section and Panel Data* (2nd ed.). Cambridge (MA): MIT Press.

Wucherpfennig, J., N. B. Weidmann, L. Girardin, L.-E. Cederman, and A. Wimmer (2011). Politically relevant ethnic groups across space and time: Introducing the GeoEPR dataset. *Conflict Management and Peace Science* 28(5), 423–437.

# Online Appendix: Mining for Peace

Roland Hodler \*    Paul Schaudt<sup>†</sup>    Alberto Vesperoni<sup>‡</sup>

July 2024

## Contents

<b>A</b>	<b>Mining in Sierra Leone</b>	<b>2</b>
A-1	Verifying the industrial mines of Sierra Leone . . . . .	2
A-2	Artisanal and small-scale mining (ASM) . . . . .	2
<b>B</b>	<b>Descriptive statistics and additional results for Sierra Leone-based analysis</b>	<b>6</b>
<b>C</b>	<b>External validity: West Africa</b>	<b>20</b>
C-1	External validity: Data and measures . . . . .	20
C-2	External validity: Results . . . . .	22

---

<sup>\*</sup>Department of Economics, University of St.Gallen; CEPR; CESifo; OxCarre; email: roland.hodler@unisg.ch

<sup>†</sup>Department of Economics, University of St.Gallen; email: paul.schaudt@unisg.ch.

<sup>‡</sup>Department of Political Economy, King's College London; email: alberto.vesperoni@kcl.ac.uk.

## A Mining in Sierra Leone

### A-1 Verifying the industrial mines of Sierra Leone

Our baseline set of industrial mines is identified via two main sources (see Section 2). First, the RMD database provides operational information at the deposit level for different minerals. [Table A-1](#) lists all these deposits. The six deposits with an active industrial mine in 2019 are highlighted in bold font. Second, for these six mines, we leverage the mining areas identified by [Maus et al. \(2020\)](#).

Table A-1: Mineral deposits (RMD)

Allotropes	Bagla Hills	Baomahun	Bently
Bunbana	Casierra	Chetham	Coastal Block
Ferensola	Freetown Complex	Gbangbaia	Gendema
Gori Hills	Jabwema	Kangari Hills	Kariba Kono
<b>Koidu</b>	Koidu Pipe 3	Konama-Bafi River	Kono
<b>Kono Operations</b>	Kukuna	Little Scarcies	Madina
Magna Egoli	<b>Marampa</b>	Matemu	Millennium
Mokanji	Nimini	Nimini Hills	No 12
Northwest Block	Pampana	Pampana North	Pampana River
Panguma	Plant 11	Plant 6	Rokel
Semabu	Sewa	Sewa-Bafi River	Sewa River
<b>Sierra Rutile</b>	<b>SML</b>	Sierra Leone	Sierra Leone Kimberlite
Sierra Leone SE Reg.	Sonfon	STHG Sewa River	Sula Mountains
Tongo	Tongo Fields	<b>Tonkolili</b>	Upper/Lower Sewa
Wara Wara	Zimmi		

*Notes:* The table lists the mineral deposits reported in the RMD. Deposits which are exploited as of 2019 with an industrial mine are highlighted in bold.

We conduct a background search for each of these six active industrial mines in order to confirm the location identified by [Maus et al. \(2020\)](#) (using Google Earth images), the primary commodity mined, and whether it has been operational for at least one year within our 1997-2018 sample period. The background searches are available upon request.

### A-2 Artisanal and small-scale mining (ASM)

Artisanal and small-scale mining (ASM) activities are hard to track for two reasons. First, many operations are not official (i.e., they are illegal). Second operations are relatively easy to move and can be very small (thus easily covered by trees and other vegetation). Nonetheless, some recent progress

has been made. [Couttenier et al. \(2022\)](#), for example, use machine learning and high-resolution images to track artisanal mining operations across West Africa. However, this approach can only be used in recent years (from around 2017 onwards) for which images with a resolution of 10 square meters or smaller are available. In the absence of any publicly available data, and with the potential for measurement error in mind, we proceed by generating proxies for artisanal and small-scale gold mining (ASGM) and artisanal and small-scale diamond mining (ASDM) ourselves. There is no ASM of bauxite, iron, and rutile in Sierra Leone.

### **A-2.1 Artisanal and small-scale gold mining (ASGM)**

To proxy for ASGM-based local resource rents, we rely on “The ASGM Overview of Sierra Leone” ([Ronkainen et al., 2019](#)). The report is the only publicly available information on ASGM covering the entire country. It lists in its supplementary material the number of ASGM sites per chiefdom in 2018. We aggregate these numbers to the level of wards. To compute ASGM-based local resource rents, we use these numbers as an imperfect proxy for the scale of gold mining activity per ward and assign the centroid of the ward as the location of the mines. Given the lack of further information, we assume that the distribution of ASGM activities remains proportional over time (i.e., if a ward has twice as many ASGM sites as another ward in 2018, then we assume that this former ward generates twice as much gold export revenues in all years), which is unlikely to hold. Moreover, using the ward centroids as point coordinates to distribute gold export revenues in proportion to the number of mines further introduces some error. In summary, there is some measurement error in our measure of ASGM-based local resource rents, but we do not have any evidence that this error is systematic.

### **A-2.2 Artisanal and small-scale diamond mining (ASDM)**

To incorporate ASDM in the computation of the local resource rents, we rely on [Zulu and Wilson \(2009\)](#), who analyze the effect of the Kimberley Process (which aims to classify conflict diamonds and reduce trade therein) on civil conflict in Sierra Leone. They highlight that most traditional ASDM areas are in the kimberlite belts in Sierra Leone, where ASDM takes place mostly in the river deltas. Panel A of [Figure A-1](#) shows these alluvial diamond mining areas along the kimberlite belts as depicted in [Zulu and Wilson \(2009\)](#).

Based on this classification, we manually delineate ASDM areas in those belts based on current (spring 2022) Google Earth images. Panel B of [Figure A-1](#) plots the distribution of the industrial diamond mines (in blue) and

Figure A-1: Kimberlite belts and mining distribution

(A) Kimberlite belts



(B) Industrial and ASDM distribution

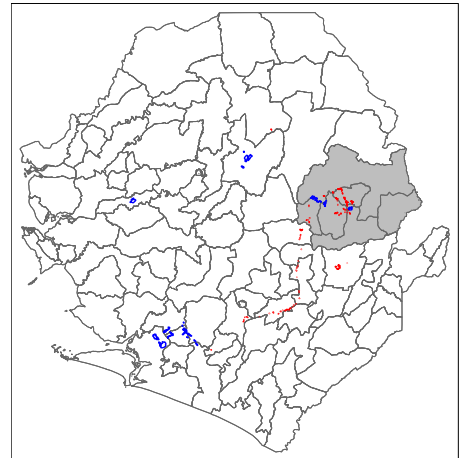


Figure 1. Map of Sierra Leone and locations of known diamond deposits (source: adapted from PAC, 2005, page 3).

*Notes:* Panel A of the figure depicts figure 1 from [Zulu and Wilson \(2009\)](#). Panel B provides a Map of Sierra Leone depicting the industrial mines as identified by [Maus et al. \(2020\)](#) in blue and the manually coded ASDM area in red. The Kono district is highlighted in grey.

the additional ASDM areas (in red). As discussed in [Zulu and Wilson \(2009\)](#), most ASDM areas are located in the Kono district (highlighted in grey), which also hosts large industrial mines.

Similar to the ASGM case, we only have a cross-sectional snapshot of ASDM areas and again assume that the general distribution of ASDM revenues does not change over time. It is, however, a bit more complicated to distribute the net export values than in the ASGM case, because of the existence of industrial diamond mines. Different sources suggest different production shares of the mine types, with the shares from ASDM ranging from 39 to 75 percent ([Zulu and Wilson, 2009](#); [Wilson, 2013](#); [Fanthorpe and Gabelle, 2013](#); [Conteh and Maconachie, 2021](#)). The inclusion of ADSM in the computation of the (diamond-based) resource rents will again introduce noise. However, given that most ASDM are located close to the industrial diamond mines, the distortion should not matter too much because the relative proximity of the different wards to the diamond mines remains relatively stable. Hence, it is no big surprise that the results remain similar if we include ASDM in the computation of the local resource rents (see Section

3.1.4 and [Figure B-6](#)), and that they do not depend on whether the share of annual net diamonds exports resulting from ASDM is assumed to be 39 or 75 percent.

## B Descriptive statistics and additional results for Sierra Leone-based analysis

Table B-1: Summary statistics

Variable	Mean	SD	Min	Max	N
<i>Panel A: Cross-sectional sample</i>					
Relative resource rents	0.01	0.02	0.00	0.10	107
Diversity among discordant groups	0.34	0.30	0.04	1.76	107
Log observed conflict exposure	-5.51	0.65	-6.33	-3.00	107
Log predicted conflict exposure	-7.04	1.18	-9.13	-2.63	107
Log population (2004)	10.57	0.50	9.53	12.67	107
Log area	5.93	1.61	-0.23	7.97	107
<i>Panel B: Panel sample</i>					
Log observed conflict exposure	-5.51	1.04	-7.43	-0.81	2,354
Log predicted conflict exposure	-7.04	1.68	-11.24	-0.16	2,354
Log bauxite proximity $\times$ log bauxite price	-41.58	6.24	-50.90	-10.82	2,354
Log diamond proximity $\times$ log diamond price	-24.96	4.25	-30.48	-7.91	2,354
Log iron proximity $\times$ log iron price	-20.74	5.07	-32.06	-3.34	2,354
<i>Panel C: Time-series sample</i>					
Share of wards in conflict	0.15	0.22	0.01	0.77	22
Peace deficit in percent of GDP	1.03	1.23	0.12	5.05	22

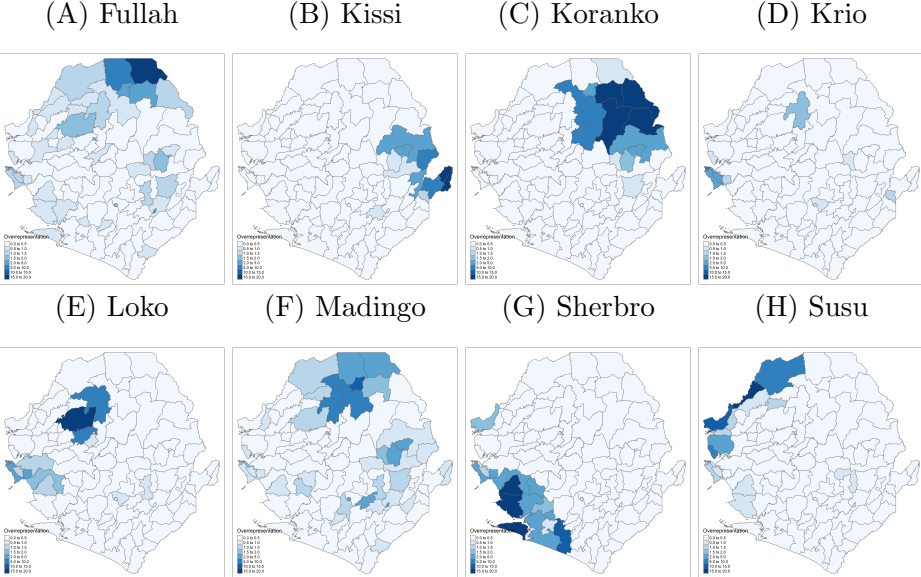
*Notes:* This table reports the summary statistics for the ward-level variables used in Figure 5, Table I (panel A), and Table II.

Table B-2: Summary statistics for variables in appendix figures and tables

Variable	Mean	SD	Min	Max	N
<i>Panel A: Cross-sectional sample</i>					
Log observed conflict exp. (all events)	-5.48	0.65	-6.20	-2.97	107
Log observed conflict exp. (excl. battles)	-5.51	0.70	-6.23	-2.82	107
Log observed conflict exp. (excl. riots)	-5.51	0.65	-6.22	-2.96	107
Log observed conflict exp. (excl. civilians)	-5.48	0.61	-6.17	-3.16	107
Log observed conflict exp. (excl. explosions)	-5.48	0.65	-6.21	-2.97	107
Log observed conflict exp. (excl. protests)	-5.46	0.64	-6.20	-2.99	107
Log observed conflict exp. (excl. deployment)	-5.51	0.65	-6.33	-2.99	107
Log observed conflict exp. (excl. government)	-5.54	0.66	-6.27	-2.96	107
Log observed conflict exp. (excl. rebels/militias)	-5.62	0.75	-6.44	-2.72	107
Log observed conflict exp. (excl. rioters/civilians)	-5.45	0.36	-6.02	-4.16	107
Log predicted conflict exp. (large groups)	-7.19	1.68	-10.31	-1.80	107
Log predicted conflict exp. (incl. ASM)	-7.00	1.20	-9.22	-3.16	107
Log predicted conflict exp. (light-weighted)	-7.07	1.17	-9.40	-2.71	107
Log relative resource rents	-5.38	0.63	-6.04	-2.81	107
Log resource rents	8.10	0.75	7.40	11.25	107
Share ethnic group of leader	0.01	0.01	0.00	0.03	107
Share of pop. politically included ward (EPR)	0.48	0.17	0.01	0.63	107
<i>Panel B: Panel sample</i>					
Log observed conflict exp. (all events)	-5.48	1.02	-7.29	-0.81	2,354
Log observed conflict exp. (excl. battles)	-5.51	1.05	-7.27	-1.56	2,247
Log observed conflict exp. (excl. riots)	-5.51	1.04	-7.31	-0.81	2,354
Log observed conflict exp. (excl. civilians)	-5.48	1.02	-7.29	-0.81	2,354
Log observed conflict exp. (excl. explosions)	-5.48	1.03	-7.29	-0.81	2,354
Log observed conflict exp. (excl. protests)	-5.46	1.02	-7.17	-0.81	2,354
Log observed conflict exp. (excl. deployment)	-5.51	1.04	-7.43	-0.81	2,354
Log observed conflict exp. (excl. government)	-5.54	1.07	-7.43	-0.81	2,354
Log observed conflict exp. (excl. rebels/militias)	-5.62	1.09	-7.43	-1.11	2,247
Log observed conflict exp. (excl. rioters/civilians)	-5.45	0.99	-7.43	-0.66	1,926
Log predicted conflict exp. (large groups)	-7.19	2.32	-12.20	1.06	2,354
Log predicted conflict exp. (light-weighted)	-7.07	1.67	-11.27	0.89	2,354
Log predicted conflict exp. (incl. ASM)	-7.00	1.72	-11.25	-0.17	2,354
Log relative resource rents	-5.38	0.83	-6.40	-1.25	2,354
Log resource rents	8.10	0.87	6.82	12.60	2,354
Mine ward $\times$ log mineral price	0.17	0.52	0.00	2.09	2,354
Share ethnic group of leader	0.01	0.02	0.00	0.08	2,354
Share of pop. politically included ward (EPR)	0.48	0.42	0.00	1.00	2,354

*Notes:* This table reports the summary statistics for variables only used in figures and tables presented in the Online Appendix.

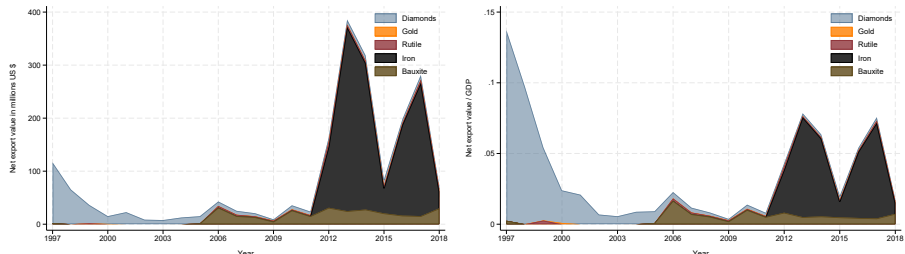
Figure B-1: Local over-representation of eight small ethnic groups



*Notes:* This figure complements Figure 4 by plotting the local over-representation ( $s_l^g/g^g$ ) across wards for the eight smaller ethnic groups in our sample, with national-level population shares ranging from 1.4–4.2 percent.

Figure B-2: Net exports of different minerals

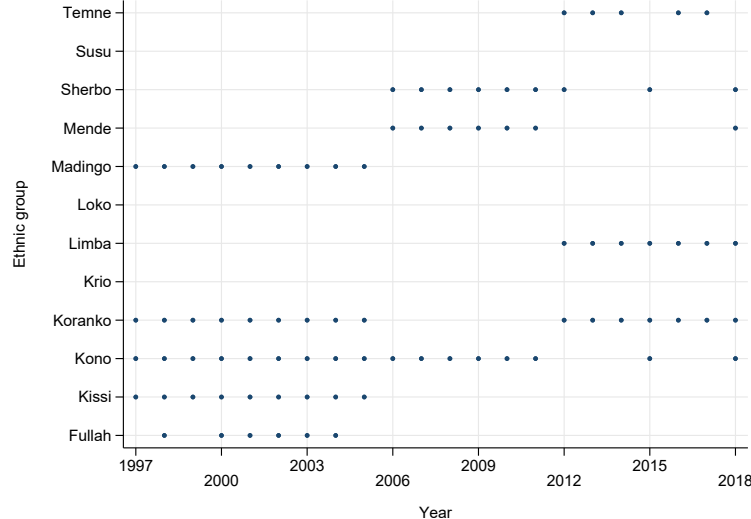
(A) Net exports in million USD (B) Net exports as a share of GDP



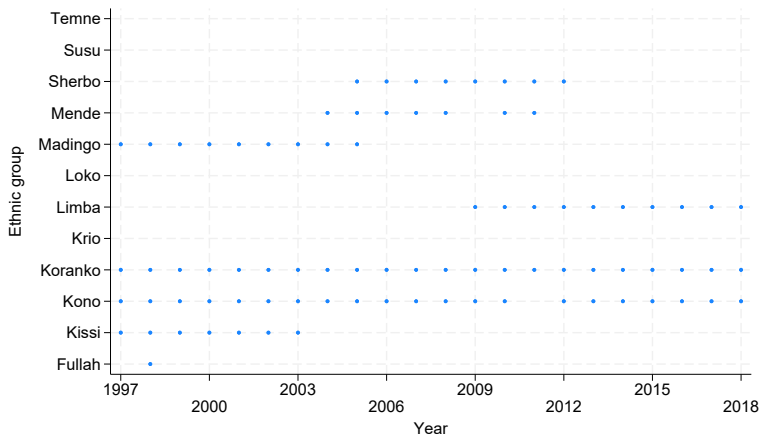
*Notes:* This figure plots the value of the net exports relative to GDP in current prices for each of the five main minerals mined in Sierra Leone over time. GDP data are from the World Bank.

Figure B-3: The set of discordant groups over time

(A)  $G^*$



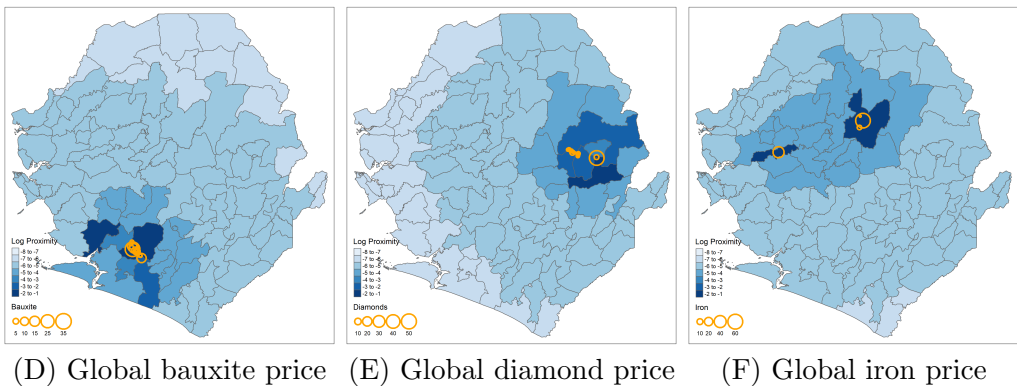
(B)  $\hat{G}^*$



*Notes:* This figure plots the set of discordant groups  $G^*$ , indicated by blue dots, for each year of our sample period. This set is determined based on Equation 3 and the data introduced in Section 2. Panel A uses the calculated relative resource shares to define  $G^*$ , panel B uses the instrumented relative local resource rents to define  $\hat{G}^*$ .

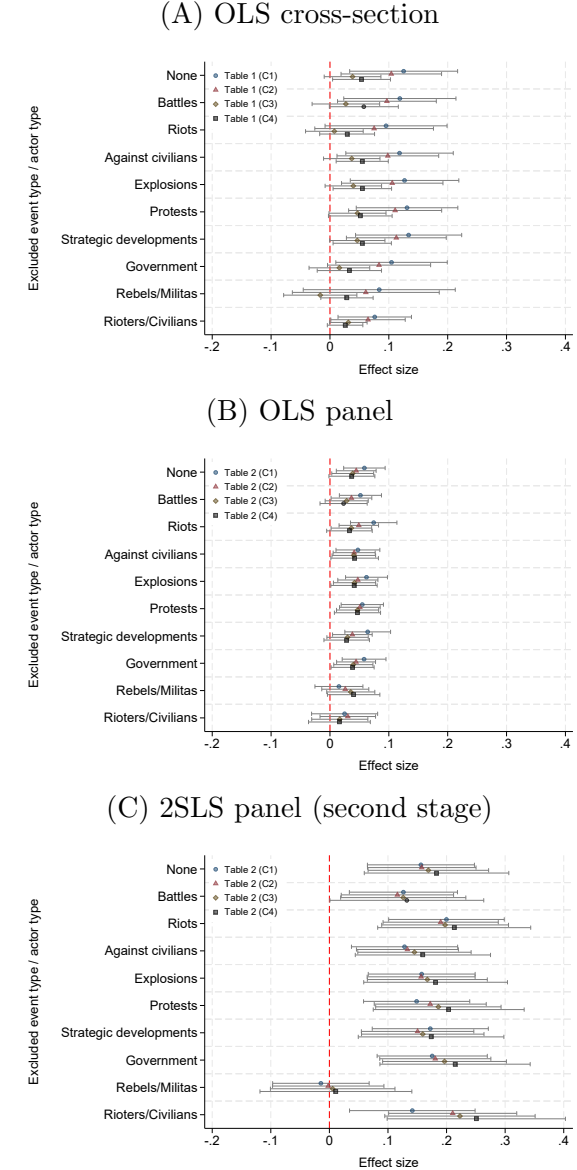
Figure B-4: Components of the instrumental variables

(A) Proximity to bauxite (B) Proximity to diamond (C) Proximity to iron  
mines mines mines



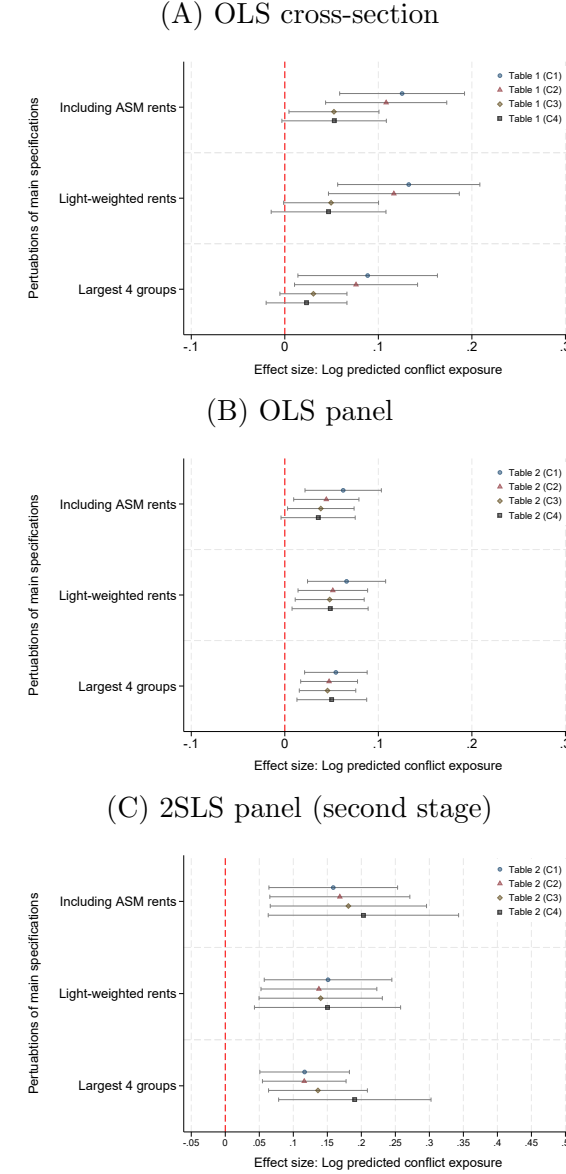
Notes: Panels A–C plot the log of the proximity of each ward to the (area-weighted) mines for bauxite, diamonds, and iron. Panels D–F plot the global prices of these minerals over time.

Figure B-5: Alternative outcome variables



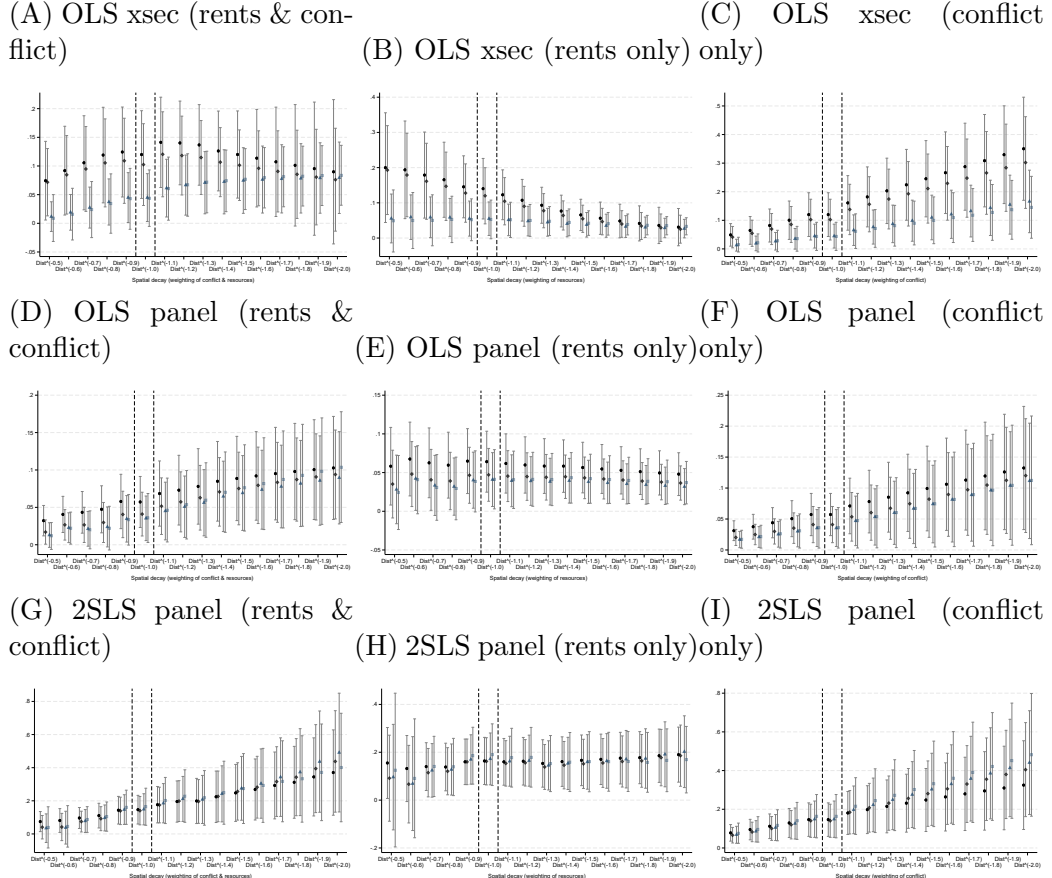
*Notes:* This figure replicates the main results reported in Table I and Table II using alternative measures of observed conflict exposure. The top row includes all ACLED event types. Rows 2–7 exclude one single event type: battles in row 2, riots in row 3, violence against civilians in row 4, explosions in row 5, protests in row 6, and strategic developments in row 7. Rows 8–10 exclude events for distinctive actor groups (ACLED actor types): State forces in row 8, rebels/militias in row 9, and civilians/protesters and rioters in row 10. Panel A follows panel A of Table I, and panels B and C follow panels A and B of Table II. The different colors and shapes of the point coefficients refer to the different specifications used in columns (1)–(4) of Table I and Table II. The 95% confidence intervals are depicted as grey bars and based on spatially clustered Conley standard errors with a 100km distance cutoff.

Figure B-6: Alternative independent variables



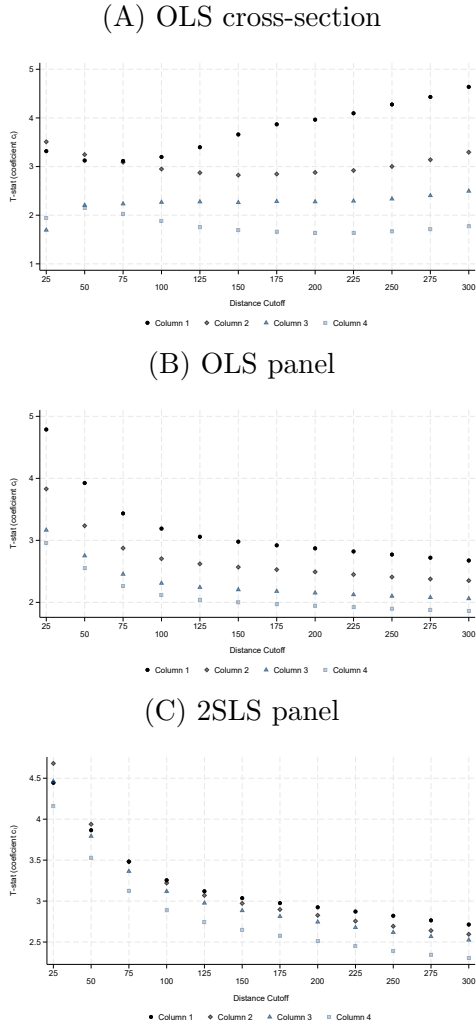
*Notes:* This figure replicates the main results reported in Table I and Table II using alternative ways to construct the predicted conflict exposure. In row 1, we construct the resource rents used in the predicted conflict exposure by weighting mining areas by light instead of area. In row 2, we construct the resource rents used in the predicted conflict exposure by including artisanal and small-scale mining (ASM, see [Section A-2](#) for details). In row 3, we only consider the ethnic population shares of the largest four ethnic groups in each ward when calculating the predicted conflict exposure. Panel A follows panel A of Table I, and panels B and C follow panels A and B of Table II. The different colors and shapes of the point coefficients refer to the different specifications used in columns (1)–(4) of Table I and Table II. The 95% confidence intervals are depicted as grey bars and based on spatially clustered Conley standard errors with a 100km distance cutoff.

Figure B-7: Alternative distance decays



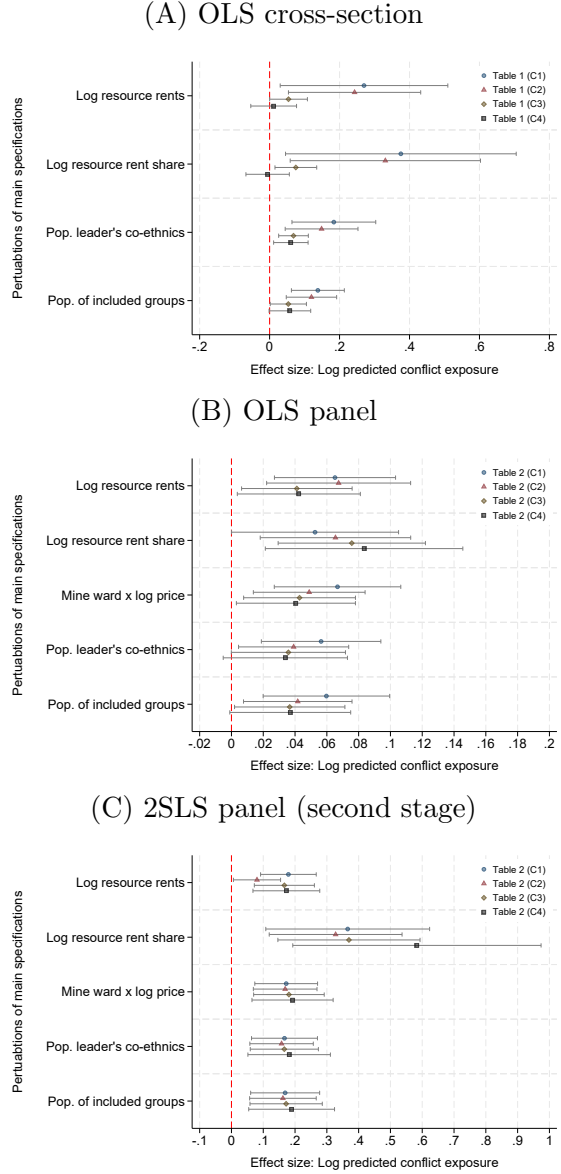
*Notes:* This figure replicates the main results reported in Table I and Table II using different distance decays, ranging from  $distance^{0.5}$  to  $distance^2$ , in the computation of both the local resource rents and the observed conflict exposure. Panel A reports the cross-sectional results from replicating panel A of Table I for these different distance decays. Black dots report the point coefficient corresponding to column (1), grey diamonds to column (2), blue triangles to column (3), and bright blue squares to column (4). Panels B and C report results from similar replication exercises when changing the distance decay only for either the local resource rents or the observed conflict exposure. Panels D-F are analogous to panels A-C but report OLS panel results from replicating panel A of Table II. Panels G-I too are analogous to panels A-C but report second-stage 2SLS panel results from replicating panel B of Table II. The 95% confidence intervals are depicted as grey bars and based on spatially clustered Conley standard errors with a 100km distance cutoff.

Figure B-8: Alternative distance cutoffs for spatially clustered standard errors



*Notes:* This figure replicates the main results reported in Table I and Table II using different distance cutoffs, ranging from 25–300 km, in the computation of the spatially clustered Conley standard errors. Panel A plots t-statistics for our main coefficient for all four columns of panel A of Table I for different distance cutoffs. Panels B and C do the same for the panel OLS and second-stage 2SLS results reported in panels A and B of Table II. In all cases, we impose a linear decline in the spatial dependence structure (using the Bartlett option in the acreg package by Colella et al. (2023)).

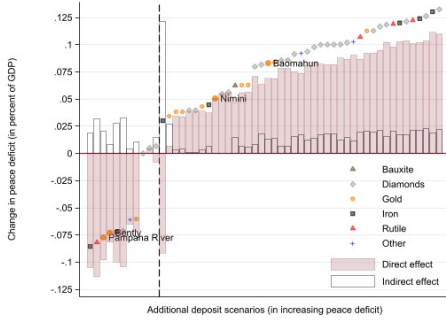
Figure B-9: Ward-level control variables



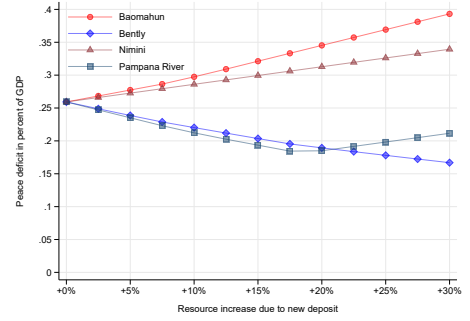
*Notes:* This figure replicates the main results reported in Table I and Table II after adding ward-level control variables. These control variables include, from top to bottom, the log of (absolute) local resource rents  $r_l$ , the log of relative local resource rents  $r_l/r$ , the interaction of an indicator variable for the presence of a mine and the log of the global price of the main mineral extracted in this ward (as in [Berman et al., 2017](#), except for panel A), the population share of the current political leader's co-ethnics, and the population share of politically included ethnic groups (according to [Wucherpfennig et al., 2011](#)). Panel A follows panel A of Table I, and panels B and C follow panels A and B of Table II. The different colors and shapes of the point coefficients refer to the different specifications used in columns (1)–(4) of Table I and Table II. The 95% confidence intervals are depicted as grey bars and based on spatially clustered Conley standard errors with a 100km distance cutoff.

Figure B-10: Predicted effects of new mines of different sizes on conflict

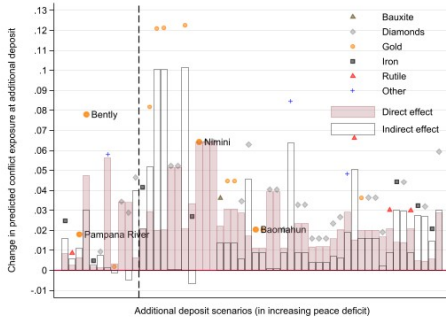
(A) Peace deficit: all deposits, 20 percent revenues



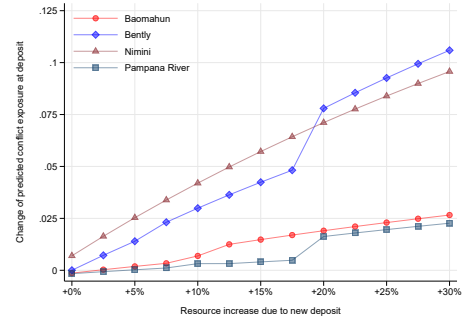
(B) Peace deficit: 4 gold deposits, different revenues



(C) Local conflict exposure at deposits: all deposits, 20 percent revenues

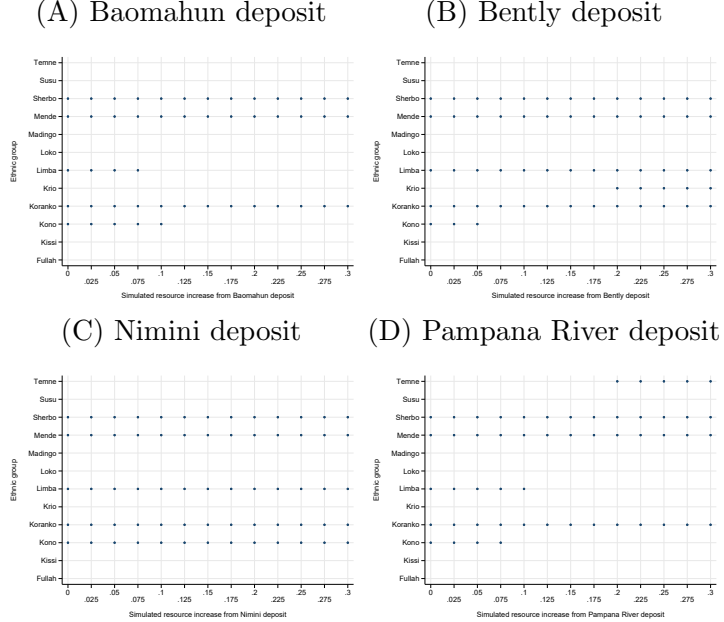


(D) Local conflict exposure at deposits: 4 gold deposits, different revenues



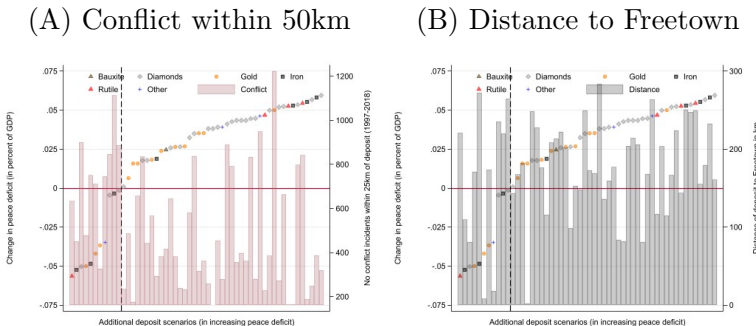
*Notes:* This figure accompanies panel B of Figure 7 and panel A of Figure 8. Panel A plots the change in the peace deficit (in percent of GDP) for simulated revenues equal to 20 percent of all existing mines combined for all known deposits. Panel B plots the change in the peace deficit (in percent of GDP) for different simulated revenues for four selected gold deposits. Panel C plots the change in the local conflict exposure for simulated revenues equal to 20 percent of all existing mines combined for the wards of all the known deposits. Panel D plots the change in the local conflict exposure for different simulated revenues in the wards where four selected gold deposits are located. In panels A and C, different colors and shapes represent the total effects for different minerals. The red bars represent direct effects (keeping the set of discordant groups fixed) and the white bars indirect effects due to the change in the set of discordant groups.

Figure B-11: The set of discordant groups for new mines of different sizes



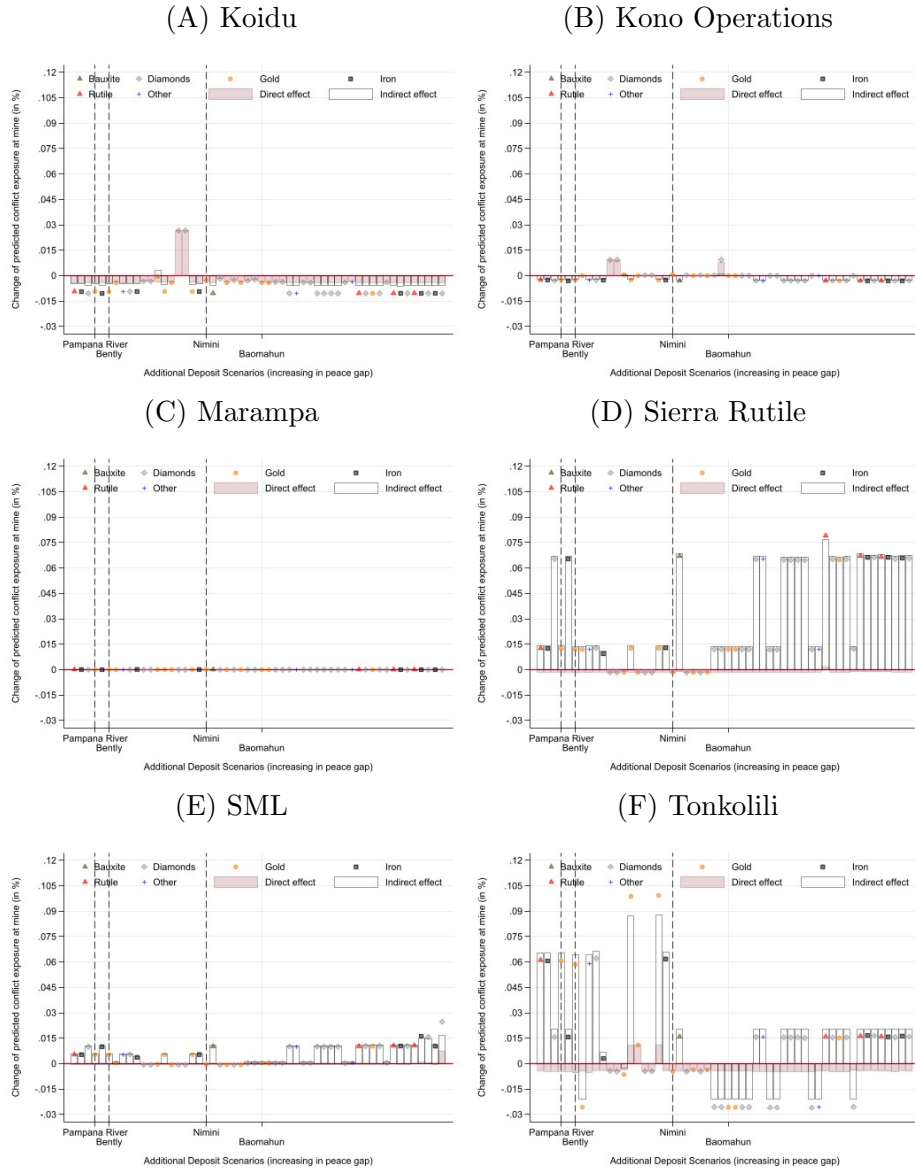
*Notes:* This figure accompanies [Figure B-10](#). Panels A–D report the set of discordant ethnic groups for different simulated revenues (in relation to the revenues of all existing mines combined) generated at four gold deposits. The revenues of all other mines are fixed to their 2018 values.

Figure B-12: Peace deficit and characteristics of potential new mines



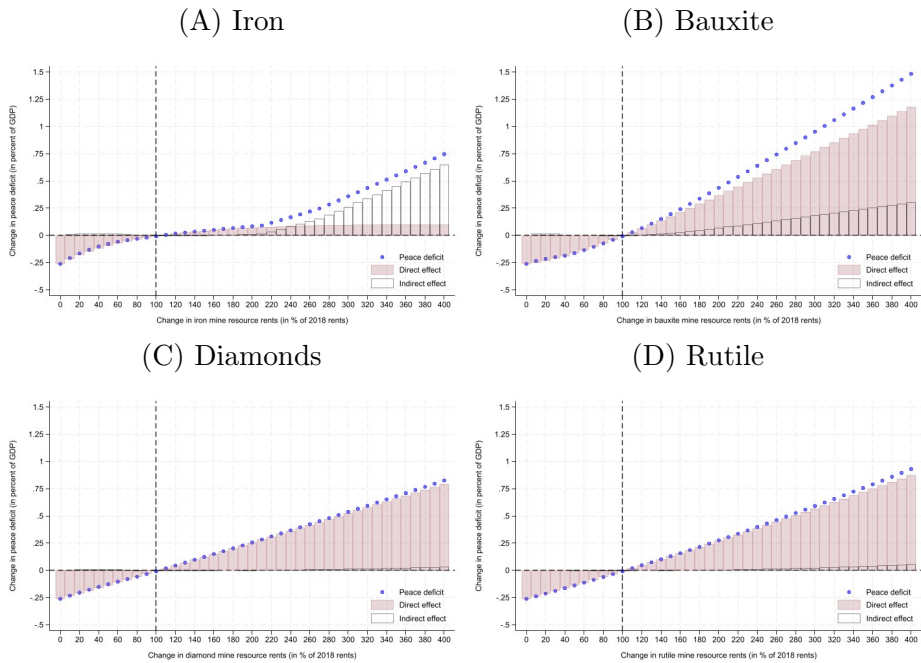
*Notes:* Both panels plot the change in the peace deficit (in percent of GDP) for simulated revenues equal to 10 percent of all existing mines combined for all known deposits (as in panel B of Figure 7). In panel A, red bars indicate the number of conflict events within 50km of the deposit from 1997–2018 (based on ACLED). In panel B, black bars indicate the distance from the deposit to Freetown (in km).

Figure B-13: Predicted effects of new mines on local conflict exposure in wards of currently active mines



*Notes:* This figure accompanies panel B of Figure 8. Panels A-F plot the change in the local conflict exposure in the wards hosting the six currently active industrial mines in Sierra Leone in response to the same simulated new mining activities as in panel B of Figure 7 and Figure 8. Different colors and shapes represent the total effects for different minerals. The red bars represent the direct effects (keeping the set of discordant groups fixed), and the white bars represent the indirect effects due to the change in the set of discordant groups. The newly mined deposits are ordered by their effects on the peace deficit.

Figure B-14: Predicted changes in the peace deficit for simulated changes in mineral prices



*Notes:* This figure plots counterfactual changes in the peace deficit (blue dots) for changes in mineral prices or, more generally, resource rents from different minerals in Sierra Leone. Panel A plots the change in the peace deficit for different percentage changes in iron rents (relative to 2018), panel B for bauxite rents, C for diamond rents, and D for rutile rents. The red bars represent the direct effects (keeping the set of discordant groups fixed), and the white bars represent the indirect effects due to the change in the set of discordant groups.

## C External validity: West Africa

In this appendix, we investigate the external validity of our main results in a sample of eight West African countries: Burkina Faso, Côte d'Ivoire, Ghana, Guinea, Liberia, Mali, Niger, and Sierra Leone.<sup>1</sup> The units of observation are gridcells of 0.5 degree  $\times$  0.5 degree, which corresponds to around 50km  $\times$  50km at the equator. These grid cells are provided by [Tollefson et al. \(2012\)](#) and commonly used in the recent literature on conflict (e.g., [Berman and Couttenier, 2015](#); [Berman et al., 2017](#); [McGuirk and Nunn, 2024](#); [Eberle et al., 2020](#)).

### C-1 External validity: Data and measures

*Ethnic geography and local over-representation:* In the absence of available census data, we use the Spatially Interpolated Data on Ethnicity (SIDE) by [Müller-Crepion and Hunziker \(2018\)](#) and the Global Human Settlement Layer (GHSL) to derive a proxy for the population of each ethnic group in each gridcell of each country.<sup>2</sup> SIDE provides local population shares of ethnic groups at 30 arc-second resolution, which corresponds to around one square kilometer at the equator, based on the spatial interpolation of geo-coded Demographic and Health Surveys. GHSL provides local population estimates at the same 30 arc-second resolution. We multiply the local population shares of ethnic groups (by SIDE) with the local population estimates for 1990 (by GHSL) to obtain a proxy for the local population of each group in each of these small cells. We can then compute the over-representation  $s_l^g/s^g$  of each ethnic group  $g$  in each gridcell  $l$  of each country.

*Mines and local resource rents:* We use the same data and the same methodology as described in Section 2.2.2 (with gridcells replacing wards) to compute the local resource rents  $r_l$  in each gridcell  $l$ , country, and year. Panel A of [Figure C-1](#) shows the resulting spatial distribution of the time-averaged relative local resource rents  $r_l/r$  within each country.

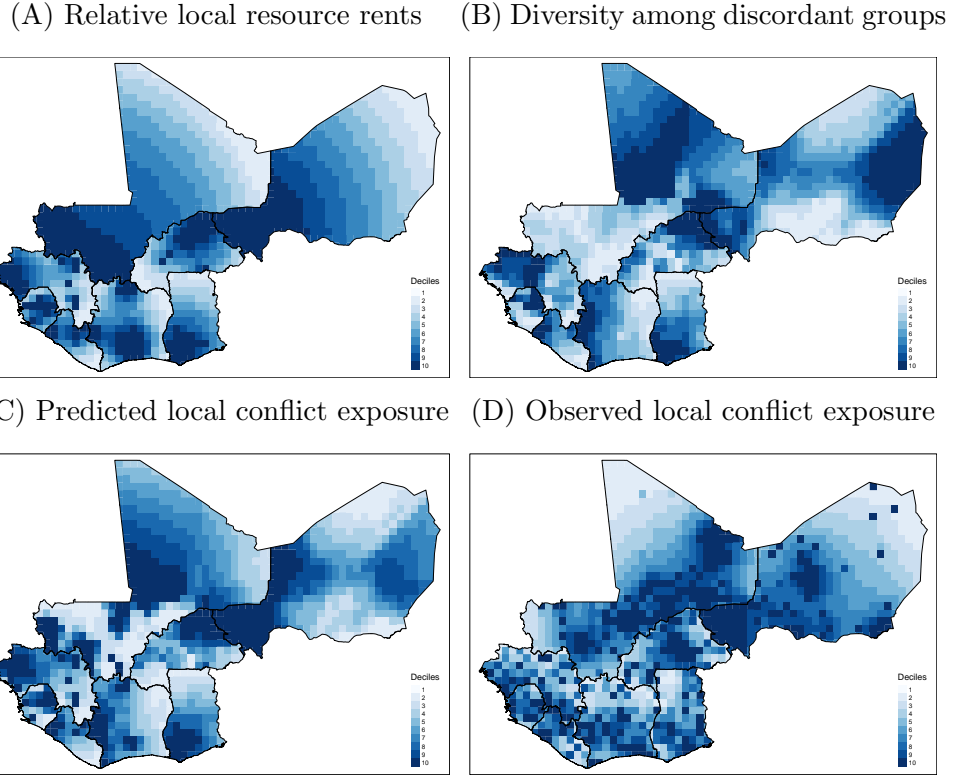
*Predicted local conflict exposure:* We derive the predicted local conflict exposure  $e_l$ , defined in Equation 5, in four steps: First, we determine the set of discordant groups in each country and year. Second, we determine the ethnic diversity among discordant groups  $D_{l,G^*}$  in each gridcell, country, and

---

<sup>1</sup>These are all West African countries for which the data on ethnicities introduced below are available *and* for which the Raw Material Data (RMD) report industrial mines that are active during our sample period from 1997–2018.

<sup>2</sup>The GHSL is constructed by the Joint Research Centre and the Directorate General for Regional and Urban Policy of the European Commission. It is publicly available at <https://ghsl.jrc.ec.europa.eu>.

Figure C-1: External validity: Resources, diversity, and conflict exposure across gridcells



*Notes:* This figure plots time-averaged values of key variables across the gridcells of each of the eight West African countries in our sample, with darker colors representing values in higher deciles. Panel A plots the relative local resource rents  $r_l/r$ , panel B the ethnic diversity among discordant groups  $D_{l,G^*}$ , panel C the predicted local conflict exposure  $e_l$ , and panel D the observed local conflict exposure.

year. Panel B of [Figure C-1](#) plots the time-averaged values of this diversity measure in space. Third, we use this diversity measure and the relative local resource rents to compute the predicted local conflict exposure  $e_l$  in each gridcell, country, and year. Finally, we average the predicted local conflict exposure  $e_l$  in each gridcell and country over the entire sample period, leading to the spatial distribution of the predicted local conflict exposure shown in Panel C of [Figure C-1](#).

*Observed local conflict exposure:* We use the same data and the same methodology as described in Section 2.2.3 (with gridcells replacing wards) to compute the observed local conflict exposure in each gridcell, country, and year. Panel D of [Figure C-1](#) shows the spatial distribution of the time-averaged

observed local conflict exposure.

## C-2 External validity: Results

We now test whether the positive and statistically significant elasticity of observed local conflict exposure with respect to predicted local conflict exposure also holds in this new sample. Panel A of Table C-1 shows that our main cross-sectional results broadly hold for Sierra Leone and West Africa. In fact, the point estimates for Sierra Leone are similar to our main results reported in Table I (panel A). The point estimates for West Africa are about half the size. Panel B shows results when limiting the analysis to politically relevant ethnic groups based on the ethnic power relation (EPR) data by [Wucherpfennig et al. \(2011\)](#). The point estimates converge somewhat between the two samples.

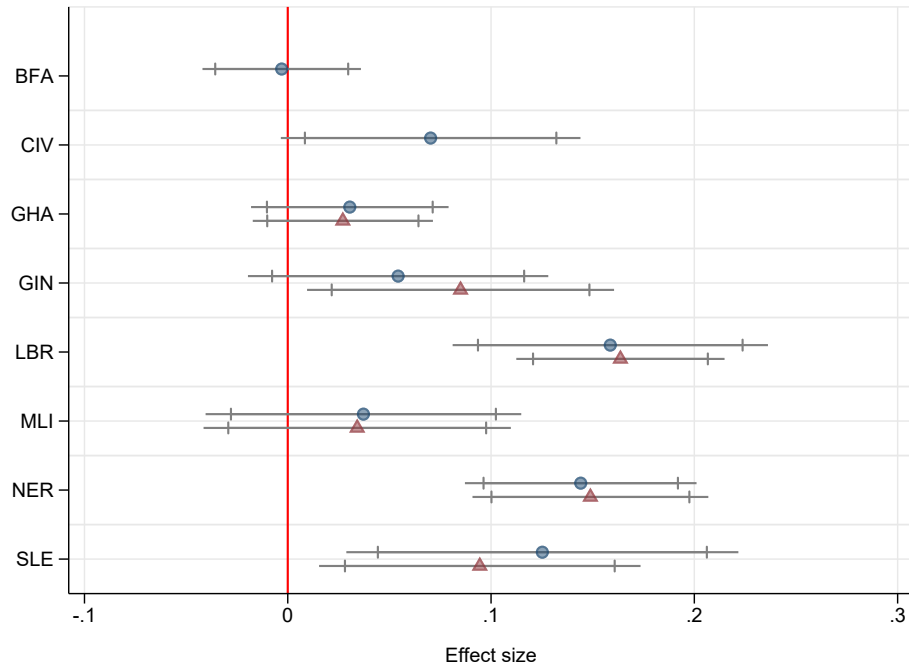
Table C-1: External validity

	<i>Dependent variable:</i>			
	<i>Log observed conflict exposure</i>			
	<i>Sierra Leone</i>	<i>West Africa</i>	(1)	(2)
<i>Panel A: All ethnic groups</i>			(3)	(4)
Log predicted conflict exposure	0.121 (0.059)	0.150 (0.053)	0.074 (0.015)	0.061 (0.013)
Obs.	39	39	1534	1534
<i>Panel B: Politically relevant ethnic groups</i>				
Log predicted conflict exposure	0.103 (0.040)	0.117 (0.040)	0.090 (0.015)	0.090 (0.015)
Obs.	39	39	1275	1275
Population and area controls	–	✓	–	✓
Country-fixed effects	✓	✓	✓	✓

*Notes:* This table reports the results of regressing the log of observed local conflict exposure on the log of predicted local conflict exposure ( $e_l$ ). Population and area controls are log of gridcell population in 1975 based on GHSL and the log of gridcell area. Columns (1)–(2) report results for Sierra Leone, and columns (3)–(4) results for our sample of eight West African countries. Panel A is based on all ethnic groups, and panel B only on ethnic groups listed as politically relevant by EPR. We cannot match EPR and SIDE groups for Burkina Faso and Côte d'Ivoire, resulting in a reduced sample in columns (3)–(4) of panel B. Standard errors are spatially clustered with a distance cutoff of 100km.

Figure C-2 reports the point estimates for each of the eight West African countries separately. We find considerable effect heterogeneity but no indication that Sierra Leone is a special case.

Figure C-2: External validity: Single-country estimates



*Notes:* This figure reports country-specific results of regressing the log of observed local conflict exposure on the log of predicted local conflict exposure in nested interaction models. The regressions include country-fixed effects and the same area and population controls as columns (2) and (4) in Table C-1. Blue dots represent point estimates when using all ethnic groups, and red triangles represent point estimates when relying solely on ethnic groups listed as politically relevant by EPR. We cannot match EPR and SIDE groups for Burkina Faso and Côte d'Ivoire, resulting in missing triangles for these countries. The 95% confidence intervals are based on spatially clustered standard errors with a distance cutoff of 100km.

## References

Berman, N. and M. Couttenier (2015). External shocks, internal shots: the geography of civil conflicts. *Review of Economics and Statistics* 97(4), 758–776. [20](#)

Berman, N., M. Couttenier, D. Rohner, and M. Thoenig (2017). This mine is mine! How minerals fuel conflicts in Africa. *American Economic Review* 107(6), 1564–1610. [15](#), [20](#)

Colella, F., R. Lalivé, S. O. Sakalli, and M. Thoenig (2023). acreg: Arbitrary correlation regression. *Stata Journal* 23(1), 119–147. [14](#)

Conteh, F. M. and R. Maconachie (2021). Artisanal mining, mechanization and human (in) security in Sierra Leone. *The Extractive Industries and Society* 8(4), 100983. [4](#)

Couttenier, M., R. S. Di, L. Inguere, M. Mohand, and L. Schmidt (2022). Mapping artisanal and small-scale mines at large scale from space with deep learning. *PLOS One* 17(9), e0267963. [3](#)

Eberle, U. J., D. Rohner, and M. Thoenig (2020). Heat and hate: Climate security and farmer-herder conflicts in Africa. Discussion Paper 15542, Centre for Economic Policy Research. [20](#)

Fan thorpe, R. and C. Gabelle (2013). *Political Economy of Extractives Governance in Sierra Leone*. World Bank. [4](#)

Maus, V., S. Giljum, J. Gutschlhofer, D. M. da Silva, M. Probst, S. L. Gass, S. Luckeneder, M. Lieber, and I. McCallum (2020). A global-scale data set of mining areas. *Scientific Data* 7(1), 1–13. [2](#), [4](#)

McGuirk, E. F. and N. Nunn (2024). Transhumant pastoralism, climate change and conflict in Africa. *Review of Economic Studies* forthcoming. [20](#)

Müller-Crepon, C. and P. Hunziker (2018). New spatial data on ethnicity: Introducing SIDE. *Journal of Peace Research* 55(5), 687–698. [20](#)

Ronkainen, J., J. De Haan, K. Anderson, and A. M. Kamara (2019). The ASGM overview of Sierra Leone. Technical report, Environment Protection Agency Sierra Leone. [3](#)

Tollefsen, A. F., H. Strand, and H. Buhaug (2012). PRIO-GRID: A unified spatial data structure. *Journal of Peace Research* 49(2), 363–374. [20](#)

Wilson, S. A. (2013). Diamond exploitation in Sierra Leone 1930 to 2010: A resource curse? *GeoJournal* 78(6), 997–1012. [4](#)

Wucherpfennig, J., N. B. Weidmann, L. Girardin, L.-E. Cederman, and A. Wimmer (2011). Politically relevant ethnic groups across space and time: Introducing the GeoEPR dataset. *Conflict Management and Peace Science* 28(5), 423–437. [15](#), [22](#)

Zulu, L. C. and S. A. Wilson (2009). Sociospatial geographies of civil war in Sierra Leone and the new global diamond order: Is the Kimberley process the panacea? *Environment and Planning C: Government and Policy* 27(6), 1107–1130. [3](#), [4](#)